Chapter 10

Layered double hydroxides and hydroxide salts: Structure and properties

Fernando Wypych (iD) **and Rilton Alves de Freitas** (iD)
Department of Chemistry, Federal University of Paraná, Centro Politécnico, Curitiba, PR, Brazil

10.1 Layered compounds: Basic concepts and nomenclature

Before describing the structures of specific layered compounds, it is important to precisely define some of the technical terms used in the following pages, based on the International Union of Pure and Applied Chemistry (IUPAC) (Work et al., 2004) and International Mineralogical Association (IMA)–International Union of Crystallography (IUCr) (Guinier et al., 1984).

– *Layered compounds*—Compounds obtained by stacking two dimensional units (layers), in which the atoms are connected prevalently by covalent bonds along the layer planes and by weak van der Waals forces along the layer packing. The layers can be neutral, cationic, or anionic and are held together by hydrogen bonding or electrostatic interactions.
– *Intercalation*—"*Process by which a substance becomes transferred into pre-existing spaces of molecular dimensions in a second substance.*" Intercalation is used for an insertion reaction that does not cause a major structural modification of the host.
– *Intercalation reactions*—"*Reaction, generally reversible, that involves the penetration of a host material by guest species without causing a major structural modification of the host.*

   Notes: Intercalation can refer to the insertion of a guest species into a one-, two-, or three-dimensional host structure. The guest species is not distributed randomly but occupies positions predetermined by the structure of the host material. Examples of intercalation reactions are the insertion of lithium into layered TiS_2 [Li_xTiS_2 ($0 \leq x \leq 1$)] and of potassium into the layers of graphite (C_8K)."

– *Intercalation compound*—"*Compounds resulting from reversible inclusion, without covalent bonding, of one kind of molecule in a solid matrix of another compound, which has a laminar structure. The host compound, a solid, may be macromolecular, crystalline or amorphous.*"
– *Delamination*—"*Process that separates the layers of a laminate by breaking their structures in planes parallel to those layers.*"
– *Exfoliation*—"*Process by which thin layers individually separate from a multilayered structure. Note: In the context of a nanocomposite material, the individual layers have at most the order of a few nanometers in thickness.*"
– *Dispersion*—"*Material comprising more than one phase where at least one of the phases consists of finely divided phase domains, often in the colloidal size range, distributed throughout a continuous phase domain.*"
– *Layered domain morphology or lamellar domain morphology*—"*Morphology in which phase domains have shapes with two dimensions much larger than the third dimension.*"
– *Polytype and polytypism*—"*An element or compound is polytypic if it occurs in several different structural modifications, each of which may be regarded as built up by stacking layers of (nearly) identical structure and composition, and where the modifications differ only in their stacking sequence. Polytypism is a special case of polymorphism: the two-dimensional translations within the layers are (essentially) preserved, whereas the lattice spacings normal to the layers vary between polytypes and are indicative of the stacking period. No such restrictions apply to polymorphism.*"
– *Polytypic transition*—"*A transition of a crystalline structure into one or more forms which differ in the way identical layers of atoms are stacked.*"
– *Turbostratic stacking*—"*Turbostratic stacking involves highly disordered (nonregular) stacking arrangements of layers where there is no registry from one layer to another, much like a stack of playing cards lying flat on each other but with no alignment of edges.*"

The structure of the minerals and synthetic materials were produced using the VESTA program (Visualization for electronic and structural analysis), version 3.4.8 (Momma and Izumi, 2011), using CIF (Crystallographic Information File) available in the Crystallography Open Database (http://www.crystallography. net/cod/).

Two layers of a generic clay mineral structure of the 2:1 group, separated by intercalated cations, were chosen as an example to define and explain the different parts of layered crystals' structure adopted throughout the text (Fig. 10.1).

These layers, independent of the complexity (from one atom of thickness in graphite and seven atoms of thickness in the present case), will be represented by a single slab (Fig. 10.2) and the single crystals will be indicated schematically by packing these slabs along the basal axis. Also, independent
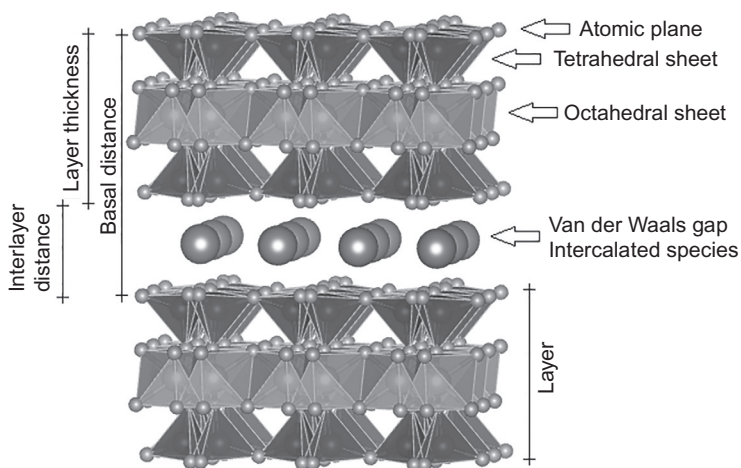
FIG. 10.1 Different parts of a hypothetical clay mineral structure of the 2:1 group.
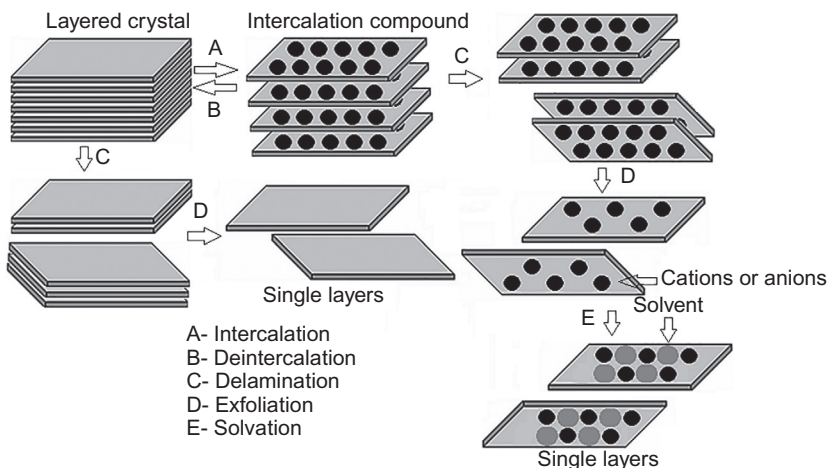

FIG. 10.2 Schematic representation of the intercalation, delamination, and exfoliation reactions of a layered crystal.

of the polytype adopted by the layered structure, the layers in the schematic representation of the single crystals used in the present text will be packed exactly on top of each other.

In a simplified way, the reactions that can be performed in a neutral lattice and can be reduced (intercalation of cations like in MoS_2) or oxidized (intercalation of anions like in graphite) are the intercalation reactions, which are normally reversible. When the layered crystal is neutral, the delamination and exfoliation reactions are not so easy and the high-energy ultrasound

equipment needs to be used, or even a mechanical peeling process. In the case of intercalation compounds, especially due to the possibility of using large charged intercalated species, the delamination and exfoliation reactions are not very difficult to process, especially if the right solvent is used. One strategy is to allow the intercalated species to be solvated so that the increased concentration of the solvent in the interlayer space will swell the crystals until the delamination/exfoliation takes place.

X-ray powder diffraction (XRPD) is one of the most powerful techniques to characterize synthesized samples, as well as single-crystal X-ray diffraction to determine the structure of minerals. XRPD is always the first technique to apply to confirm the successful synthesis of known materials, since the XRPD patterns will match the standard data stored in databases like that of the JCPDS (International Centre for Diffraction Data Sample Preparation Methods in X-Ray Powder Diffraction). When the sample has an unknown structure, the first information to be obtained is the basal distance, by analyzing the XRPD patterns. Since powders are normally composed of platelet-like sub- or micrometric particles, the sample preparation for analysis is important. It is difficult to avoid the texturization of the platelet-like particles in the sample holder, since even a small pressure will orient the crystals parallel to the sample holder, maximizing the intensity of the basal diffraction peaks (conventionally (00l)) and decreasing the intensity of the nonbasal reflections (hk0). As the basal distances (which vary according to the intercalated anion) are bigger than the bonds between the atoms in the layers, these are the first reflections to be detected and occur normally in the form of several orders, all of them reflecting the same interplanar distance, as indicated in Bragg's equation ($d(\text{Å}) = n\lambda/2\sin\theta$; λ = wavelength in Å and θ = diffraction angle in degrees; n = reflection order). To avoid the errors of the interplanar distances (d) attributed to sample displacement, the sample should be placed exactly at the surface of the sample holder, forming a uniform film and avoiding humps and depressions.

Also, due to the increased imprecision of the "d" values obtained as the diffraction peaks are delocalized to lower diffraction angles, the higher order basal reflections should be used to determine the basal distance, using Bragg's equation. Also, in the case of hexagonal structures, which are the most common structure adopted by LDH and LHS, the average distance between the two metals in the layers can be obtained from the (110) reflections (close to 62 degrees in 2θ with λ $Cu_{k\alpha}$ = 1.5418 Å) multiplied by 2 ($d_{110} \times 2$ = average M–M distance).

To correct the errors due to the vertical displacement of the sample from the center of the diffraction goniometer and the errors attributed to the reflection positions at lower diffraction angles, the corrections need to be used as recommended by Hermans et al. (2014), based on the method described by Noyan and Cohen (1987).

Another method used to characterize intercalation compounds is to detect the presence of typical functional groups through Fourier-transform infrared spectroscopy (FTIR). Here some basic precautions need to be taken. Since the common method is to use KBr pellets, the sample needs to be milled and homogeneously dispersed in KBr powder before pressing the mixture to obtain almost transparent pellets. When a mortar and pestle are used to apply extensive shared forces, the sample can be delaminated or even decomposed. Consequently, care must be taken during these analyses.

In the case of an intercalated compound, one can observe that after the exfoliation, 50% of the charged species will be attached to each detached layer, and if the species are not solvated, this solvation reaction will occur easily (Fig. 10.2). If no space is available to be occupied by the solvent in solvating the intercalated species, partial reduction of the concentration of the intercalation species can occur by oxidation, as in the case of $KMoS_2$, when after hydration the composition will be $K_{1-x}(H_2O)yMoS_2$ (Wypych and Schöllhorn, 1992; Wypych et al., 1999). The intercalated charged species (cations or anions) can be replaced by other species of interest (Fig. 10.3), always considering the stoichiometry of the reactions and the charge of species to be exchanged with the desired one (Miyata, 1983; Constantino and Pinnavaia, 1995; Newman and Jones, 1999; Sotiles and Wypych, 2019).

Single-charged intercalated species can be effortlessly replaced by double- and triple- charged species, but the opposite reactions are not easily processed, even if the concentration of the species in solution is high. In fact, to complete the exchange reactions, normally the species in solution needs to be in excess and the reactions processed under gentle stirring to avoid damaging the crystals during long exposure to stirring. Sometimes the solution needs to be replaced by a new one to achieve the complete topotactic exchange reaction.

Intermediate phases can also be obtained during the exchange reaction, when the presence of both charged species can coexist in the interlayer space and the basal distance is determined by the bigger hydrated (or anhydrous) ionic diameter of the intercalated species. X-ray diffraction, for example,
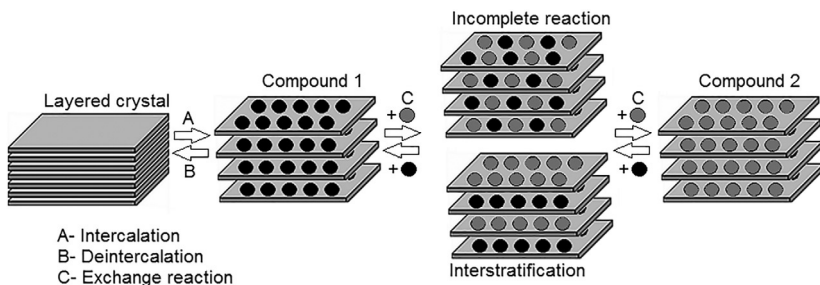

FIG. 10.3 Schematic representation of the intercalation and reversible exchange reaction of a layered crystal.

can indicate that the exchange reaction did not happen or was already completed, but other analytical techniques need to be used to certify that the exchange reaction occurred (Fig. 10.3). Interstratification is also another phenomenon that can be observed with layered materials during exchange reactions, where some interlayers are replaced by the new species while the other is not (Fig. 10.3).

During the intercalation or exchange reaction, it is also possible to obtain new polytypes, when the stacking of the layers can be changed (Fig. 10.4) by shifting or by rotation, always with regular organization.

The classification of different polytypes is based on the number of stacked layers in the basal unit cell (along the basal axis) (Booking and Drits, 1993).

Ex.: In the 1H-LDH polytypes, the unit cell contains one layer and the structure is hexagonal (the series of basal diffraction peaks will be indexed as (001), (002), (003), etc.), while in the 3R-LDH polytypes, the unit cell contains three layers and the structure is rhombohedral (the series of basal diffraction peaks will be indexed as (003), (006), (009), etc.). Recently the first 9R zincalstibite polytype has been reported in the literature (Mills et al., 2012a).

When the layers are randomly oriented relative to each other and not regularly packed, rotation stacking faults are normally observed, an effect known as turbostraticity or rotational stacking disorder. This effect is normally observed when the layered crystals are exfoliated and the layers are restacked after removal of the solvent or by precipitation, or even after extensive swelling, as occurs in clay minerals of the smectite group. Also, it is common to obtain different staging during the intercalation, when some interlayer's space is occupied while others remain empty. When intercalated layered crystals are exfoliated, only half of the intercalated ions will be kept on each side of the layers, and if the intercalated ions are anhydrous in the bulk, these will be solvated (hydrated in the case of water) at both sides of the single layers (Fig. 10.5).
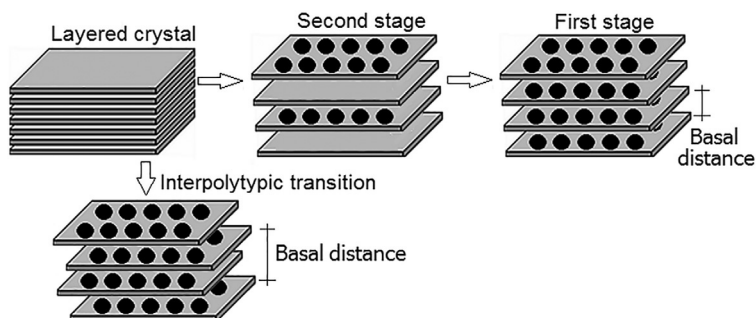

FIG. 10.4 Schematic representation of the stage formation and interpolytypic transition during intercalation.
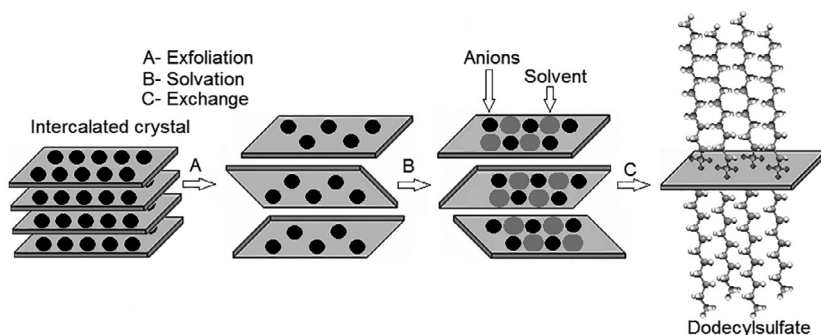
FIG. 10.5 Schematic representation of some reactions possible in layered compounds.
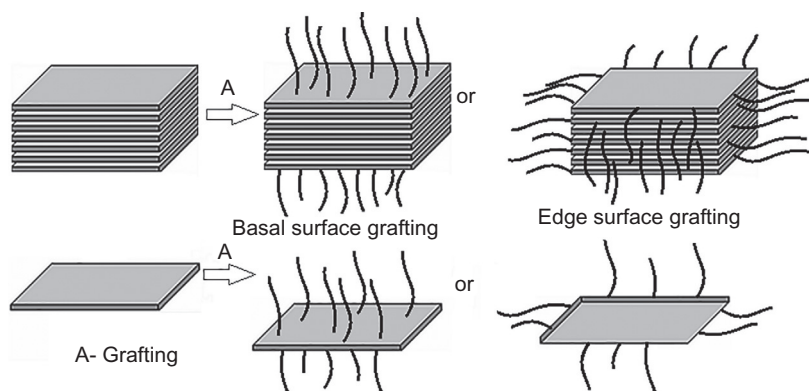

FIG. 10.6 Schematic representation of the surface chemical grafting of a layered crystal or single layers.

The intercalated species can be replaced by organic species (in the present case, intercalated anions were replaced by dodecylsulfate ($C_{12}H_{25}SO_4^-$), an anionic surfactant), consequently changing the polarity of the layers. Other reactions that can be performed in neutral or intercalated layered compounds where the bulk is delaminated or exfoliated are surface grafting reactions (Fig. 10.6), when new functional groups are attached to the surface (Wypych and Satyanarayana, 2005; Wypych et al., 2018). Chemical functionalization of the basal or edge surface can be obtained, or even of both surfaces simultaneously.

This kind of reaction is very important when the surface polarity needs to be changed to disperse, for example, a hydrophilic layered material in a hydrophobic polymer or solvent (Wypych et al., 2018). The right grafted functional groups need to be chosen, and even at very low concentration, the surface polarity can be changed. After defining these basic concepts and nomenclature used in the analysis of layered materials, in the following

parts of the chapter, a special class of layered materials composed of layered double hydroxides (LDH) and layered hydroxide salts (LHS) is introduced and described.

10.2 Layered double hydroxides

10.2.1 Layered double hydroxides with the composition $[M_{1-x}^{2+}M_x^{3+}(OH)_2] (A^{n-})_{x/n} \cdot yH_2O$
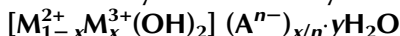
Layered double hydroxides (LDH) are a class of natural or synthetic materials which are in the majority of cases based on the structure of cadmium iodide (CdI_2), but also based on the structure of the mineral brucite or magnesium hydroxide ($Mg(OH)_2$) and other divalent transition metal hydroxides, like Mn, Ni, Co, Fe, Cd, etc. The structure of brucite is composed of slightly distorted octahedral units of $Mg(OH)_6$, which share edges to form two-dimensional layers, which are stacked along the "c" direction (basal axis) and held together by van der Waals forces (Fig. 10.7). Since all the octahedral positions are occupied, the structure is classified as trioctahedral.

Using Pauling's electroneutrality principle of the structure, each Mg^{+2} is coordinated to 6 OH^- groups sharing $2^+/6 = +1/3$ of the positive charge with each OH^- group and each OH^- sharing the negative charge with other Mg^{+2} cations ($-1/3$). These layered crystals, grown preferentially along the "a" and "b" axis, give to this material a high aspect ratio, which is determined by the ratio of the diameter of the layered particles along the platelet planes to the thickness along the basal direction, normally perpendicular to the platelet particles (Feitknecht and Gerber, 1942; Crepaldi et al., 1999; Rives, 2001; Wypych and Satyanarayana, 2004; Duan and Evans, 2006; Guo et al., 2010; Wang and O'Hare, 2012; Sherman, 2015).

The name layered double hydroxide is related to the composition of the materials, which are composed of two different metals, where the main one has oxidation state 2+, such as Mg^{2+} in brucite's structure, and the one that will partially isomorphically substitute M^{2+} from the structure has 3+ oxidation state. The partial substitution generates the chemical composition
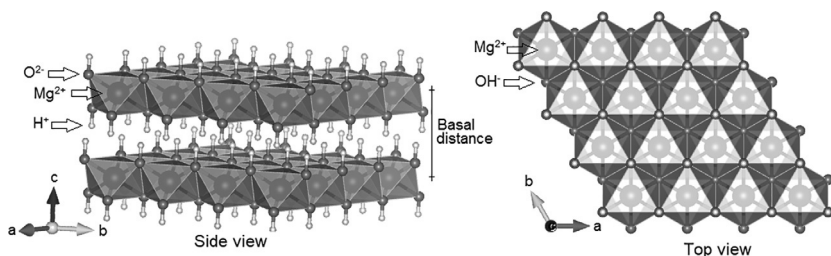

FIG. 10.7 Schematic polyhedral representation of brucite ($Mg(OH)_2$), along the indicated axis (Zigan and Rothbauer, 1967).

$[M^{2+}_{1-x}M^{3+}_x(OH)_2]^{x+}$ in the layers, where the positive charge needs to be compensated by intercalated anions $(A^{n-})_{x/n} \cdot yH_2O$. The values of "$x$" usually vary from $0.33 < x < 0.80$, which gives the molar ratios $M^{2+}:M^{3+}$ from 2:1 to 4:1. The most representative LDH family has the formula $[M^{2+}_{1-x}M^{3+}_x(OH)_2]$ $(A^{n-})_{x/n} \cdot yH_2O$, where $[M^{2+}_{1-x}M^{3+}_x(OH)_2]^{x+}$ represents the layer domain and $(A^{n-})_{x/n} \cdot yH_2O$ denotes the interlayer domain. In LDH compositions, M^{2+} metals are normally represented by Mg, Ca, Sr, Mn, Fe, Co, Ni, Cu, Zn, Cd while M^{3+} are represented by Al, Cr, Fe, Sc, Ga, Y, In, Ce, and A^{n-}, with an infinity of inorganic and organic anions.

This first group of LDH can be represented by the structure of manasseite, with the composition $[Mg_4Al_2(OH)_{12}(CO_3) \cdot 3H_2O]$ (Fig. 10.8) (Arakcheeva et al., 1996), but many other minerals, like hydrotalcite ($Mg_6Al_2CO_3(OH)_{16} \cdot 4H_2O$), quintinite ($Mg_4Al_2(OH)_{12}CO_3 \cdot 3H_2O$), pyroaurite ($Mg_6Fe_2^{3+}(CO_3)$ $(OH)_{16} \cdot 4H_2O$), takovite ($Ni_6Al_2(OH)_{16}(CO_3,OH) \cdot 4H_2O$), stichtite ($Mg_6Cr_2$ $(CO_3)(OH)_{16} \cdot 4H_2O$), hydrocalumite ($Ca_2Al(OH)_6(CO_3^{2-})_{0.11}(OH)_{0.78}$ $2.38H_2O$), meixnerite ($Mg_6Al_2(OH)_{16}(CO_3) \cdot 4H_2O$), dritsite ($Li_2Al_4(OH)_{12}Cl_2 \cdot 3H_2O$) (Zhitova et al., 2019), and akopovaite ($Li_2Al_4(OH)_{12}(CO_3) \cdot 3H_2O$) (Karpenko et al., 2020), have been described, just to cite some examples.

The majority of minerals are intercalated with carbonate and the $M^{2+}:M^{3+}$ molar ratio normally varies from 2:1 to 3:1, while the M^{3+} is normally aluminum (Mills et al., 2012a,b). But many exceptions have been described in the literature. It is important to mention that in synthetic LHS, the amounts of intercalated anions can be regulated by controlling the $M^{2+}:M^{3+}$ molar ratio or the "x" in the formula $[M^{2+}_{1-x}M^{3+}_x(OH)_2]$ $(A^{n-})_{x/n} \cdot yH_2O$. However, the molar ratio used will not necessarily produce the desired compound. In this case, some amorphous hydroxides can be segregated and chemical analysis will generate incongruent results.

When Fe^{2+} is oxidized in $Fe(OH)_2$, which has a similar structure of $Mg(OH)_2$, layered double hydroxides with a single metal can be obtained, denominated the green rust (GR) family, with the composition $[Fe^{2+}_{1-x}Fe^{3+}_x$ $(OH)_2](A^{n-})_{x/n} \cdot yH_2O$, where in nature, A^{n-} is normally represented by carbonate. The same can occur with $Ni(OH)_2$ and $Co(OH)_2$, where divalent
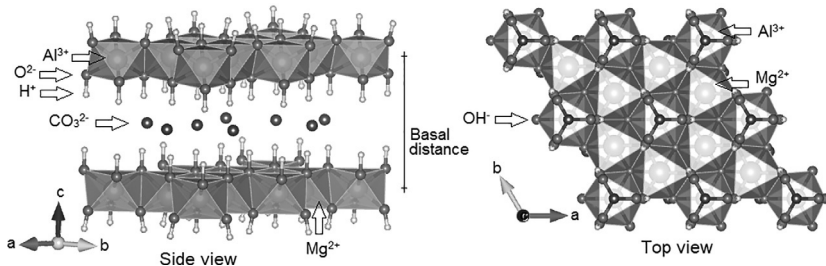

FIG. 10.8 Schematic polyhedral representation of manasseite-like LDH structure oriented along the indicated axis directions (Arakcheeva et al., 1996).

and trivalent metal cations are present in the layered structure. Ternary (and even quaternary) layered double hydroxides with the generic composition $[M_a^{2+}{}_{1-y-x}M_b^{2+}{}_yM^{3+}{}_x(OH)_2]\,(A^{n-})_{x/n}{\cdot}yH_2O$ or $[M^{2+}{}_{1-x}M_a^{3+}{}_{x-y}M_b^{3+}{}_y(OH)_2]$ $(A^{n-})_{x/n}{\cdot}yH_2O$ can also be obtained but are rarely described in the literature. The partially replaced metal in the LDH structure is normally M^{2+} and only rarely M^{3+} (Lei et al., 2013; Kühl et al., 2015; Rathee et al., 2019).

10.2.2 Layered double hydroxides with the composition $[Li(Al(OH)_3)_2](A^{n-})_{1/n}{\cdot}yH_2O$

The second group of compounds less frequently observed in layered double hydroxides is $[Li(Al(OH)_3)_2](A^{n-})_{1/n}{\cdot}yH_2O$ (Serna et al., 1982; Besserguenev et al., 1997; Uvarova et al., 2005; Hawthorne and Cooper, 2013; Britto and Kamath, 2014; Zhitova et al., 2019; Karpenko et al., 2020). These materials are not obtained by isomorphic substitution of M^{2+} by M^{3+} or by oxidation of M^{2+}, but rather by occupation of the vacant octahedral site of the aluminum hydroxide $(Al(OH)_{3-}\,Al_{2/3}\upsilon_{1/3}(OH)_2$ (υ: vacant site). They include polymorphs like gibbsite (Saalfeld and Wedde, 1974), bayerite (Rothbauer et al., 1967), nordstrandite (Saalfeld and Jarchow, 1968), and doyleite (Clark et al., 1998), with lithium cations in solid state or in solution. Gibbsite, used as example (Fig. 10.9), is classified as dioctahedral, since only 2/3 of the octahedral sites are occupied due to the 3+ oxidation of aluminum in comparison to the 2+ oxidation state of magnesium in brucite's structure.

After occupation of the vacant sites, positive charged layer domains are obtained with the composition $[Li(Al(OH)_3)_2]^+$, which need to be charge compensated by the intercalation of hydrated anions $(A^{n-})_{1/n}{\cdot}yH_2O$. Several different anions can occupy the interlayer space, like Cl^-, Br^-, NO_3^-, OH^-, SO_4^{2-}, etc. Recently, the structures have been described of two minerals, with the composition $[Li_2Al_4(OH)_{12}Cl_2{\cdot}3H_2O]$ (dritsite) (Zhitova et al., 2019) (Fig. 10.10) and the carbonate analog of dritsite $Li_2Al_4(OH)_{12}(CO_3){\cdot}3H_2O$ (akopovaite) (Karpenko et al., 2020). Akopovaite was found in the $1M$ polytype, whereas dritsite was found in the $2H$ polytype.
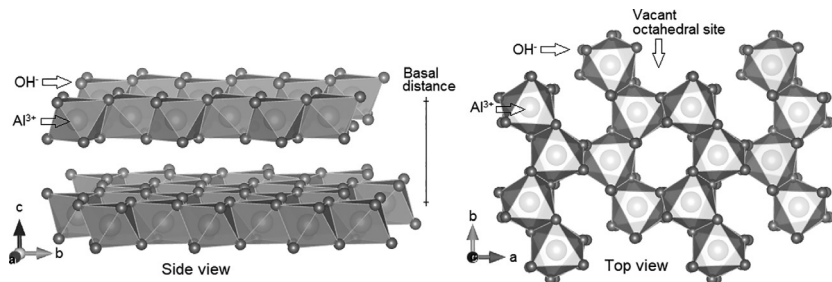

FIG. 10.9 Schematic polyhedral representation of gibbsite's $(Al(OH)_3)$ oriented along the indicated axis directions (Saalfeld and Wedde, 1974).
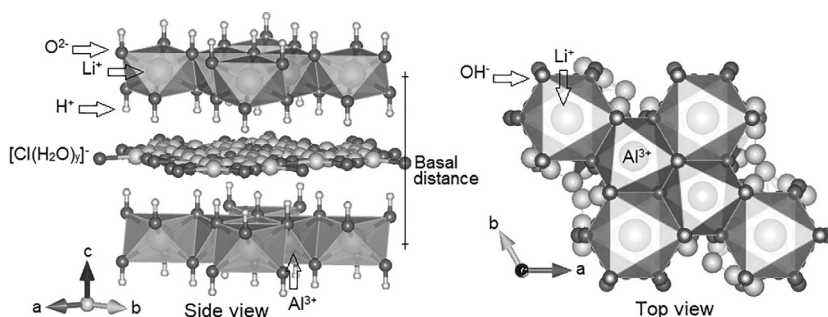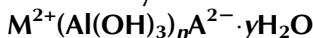
FIG. 10.10 Schematic polyhedral representation of dritsite's structure oriented along the indicated axis directions (Zhitova et al., 2019).

10.2.3 Layered double hydroxides with the composition $M^{2+}(Al(OH)_3)_nA^{2-}\cdot yH_2O$

Another compositions presented by layered double hydroxides, obtained by the occupation of the vacant octahedral sites of dioctahedral $Al(OH)_3$, are $M^{2+}(Al(OH)_3)_nA^{2-}\cdot yH_2O$ ($A^{2-}=SO_4^{2-}$, VO_3^{2-}; $M^{2+}=Ni^{2+}$, Co^{2+}, Zn^{2+} and Cu^2; $n=2$, 4), which occurs naturally in minerals or can be obtained by synthetic routes (Fogg et al., 2004; Williams et al., 2006a,b; Jensen et al., 2019; Szabados et al., 2019). These materials, also known as "aluminum-rich layered double hydroxides," are similar to those obtained after reaction with lithium salts, but where the vacant octahedral sites are occupied by divalent cations (Ni^{2+}, Co^{2+}, Zn^{2+}, and Cu^{2+} have been reported), obtaining double-positively charged layer domains $[M^{2+}(Al(OH)_3)_2]^{2+}$, which need to be charge compensated by the intercalation of hydrated anions $(A^{n-})_{1/n}\cdot yH_2O$ (as far as we know at this writing, only SO_4^{2-} and VO_3^{2-} have been reported). The minerals nickelalumite, chalcoalumite, alvanite, and kyrgyzstanite have been reported (Williams and Khin, 1971; Pertlik and Dunn, 1990; Agakhanov et al., 2005; Uvarova et al., 2005; Hawthorne and Cooper, 2013), respectively, the compositions $NiAl_4(OH)_{12}SO_4\cdot 3H_2O$, $CuAl_4(OH)_{12}SO_4\cdot 3H_2O$, (Zn,Ni) $Al_4(VO_3)_2(OH)_{12}\cdot 2H_2O$, and $ZnAl_4(SO_4)(OH)_{12}\cdot 3H_2O$. Fig. 10.11 shows the schematic polyhedral representation of nickelalumite's structure (Uvarova et al., 2005).

10.2.4 Layered double hydroxides with the composition $[M_6^{2+}Al_3^{3+}(OH)_{18}][B^+(H_2O)_6(X^{2-})_2]\cdot 6H_2O$
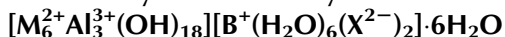
The fourth composition of layered double hydroxides is $[M_6^{2+}Al_3^{3+}(OH)_{18}]$ $[B^+(H_2O)_6(X^{2-})_2]\cdot 6H_2O$ ($M^{2+}=Mg$, Mn, Zn, Co, Ni, Cu; $B^+=Li$, Na, K, NH_4; $X^{2-}=SO_4$, HPO_4) (Rodgers et al., 1977; Rius and Plana, 1986; Zamarreno et al., 1989; Witzke et al., 1995; Cooper and Hawthorne, 1996; Huminicki and Hawthorne, 2003; Ruby et al., 2006; Christiansen et al., 2009, 2014; Sotiles and Wypych, 2019; Sotiles et al., 2019a,b).
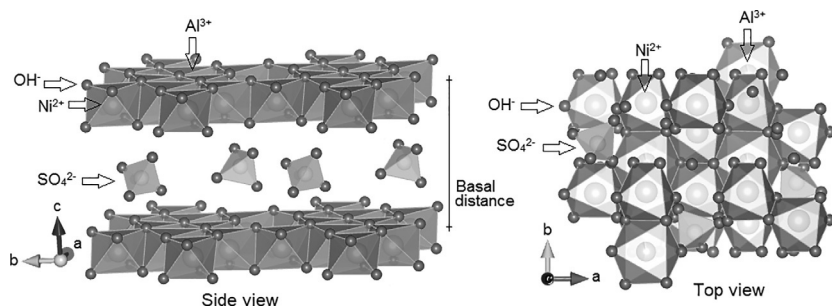
FIG. 10.11 Schematic polyhedral representation of nickelalumite's structure oriented along the indicated axis directions. Hydrogen atoms and water molecules have been removed from the structure to facilitate visualization (Uvarova et al., 2005).

Some of these compositions have already been observed in minerals, like motukoreaite ($M^{2+} = Mg$), natroglaucocerinite ($M^{2+} = Zn$), shigaite ($M^{2+} = Mn$), and nikischerite ($M^{2+} = Fe$), as well as sulfate green rusts denominated GR_{SO4} ($NaFe_6^{2+}Fe_3^{3+}(SO_4)_2(OH)_{18} \cdot 12H_2O$, $KFe_6^{2+}Fe_3^{3+}(SO_4)_2(OH)_{18} \cdot 12H_2O$) (Rodgers et al., 1977; Rius and Plana, 1986; Zamarreno et al., 1989; Witzke et al., 1995; Cooper and Hawthorne, 1996; Huminicki and Hawthorne, 2003; Zegeye et al., 2005; Ruby et al., 2006; Christiansen et al., 2009, 2014; Ahmed et al., 2010). Fig. 10.12 shows the schematic polyhedral representation of nikischerite's structure (Huminicki and Hawthorne, 2003).

Chemical modification of surfaces can be easily performed by intercalation with anionic surfactants, functionalization, or through a chemical method to obtain aqueous miscible organic layered double hydroxide (AMO-LDH) (Fig. 10.13).

After synthesizing the LDH, the particles are washed with a water miscible organic solvent and the materials with the composition $[M_{1-x}^{z+}M_x^{y+}(OH)_2]^{a+}$ $(CO_3)_{a/2} \cdot mH_2O \times n$(AMO-solvent) are obtained (Chen et al., 2014; Yang et al., 2014; Erastova et al., 2017). The particles' surfaces can be modified, changing the surface polarity from hydrophilic to hydrophobic. In this method, only the surface of the particles will be modified. This is also the case of the functionalization (Fig. 10.5), while in intercalated surfactants, both the outer and inner surfaces can be modified (Clearfield et al., 1991; Carlino, 1997; Adachi-Pagano et al., 2000; Guimarães et al., 2000; Bubniak et al., 2002; Kameda et al., 2008; Cursino et al., 2013, 2015).

One important aspect still not totally explored in the literature is the possibility to obtain pillared LDH (and also the LHS discussed in the following section) using dicarboxylic or disulfonic acid with different chain lengths to obtain organically pillared hydroxides (OPH) with different functionalities and extremely high surface areas. These have potential industrial applications, as reported for pillared clays (PILC), when the pillars are obtained by exchanging the interlayer cations with metal-hydroxy oligomeric species,
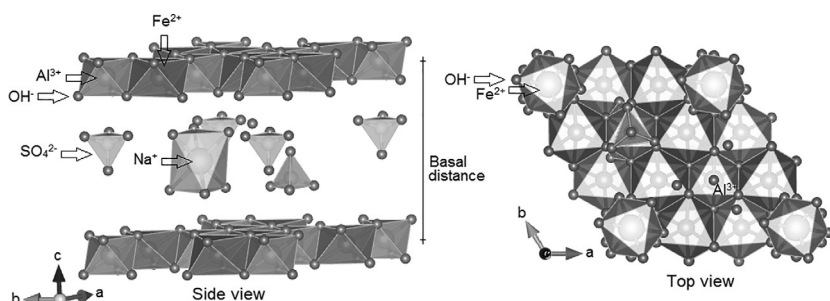
FIG. 10.12 Schematic polyhedral representation of nikischerite's structure ($[Fe_6^{2+}Al_3^{3+}(OH)_{18}]$ $[Na(H_2O)_6(SO_4)_2]\cdot 6H_2O$) oriented along the indicated axis directions. Hydrogen atoms and water molecules have been removed from the structure to facilitate visualization (Huminicki and Hawthorne, 2003).
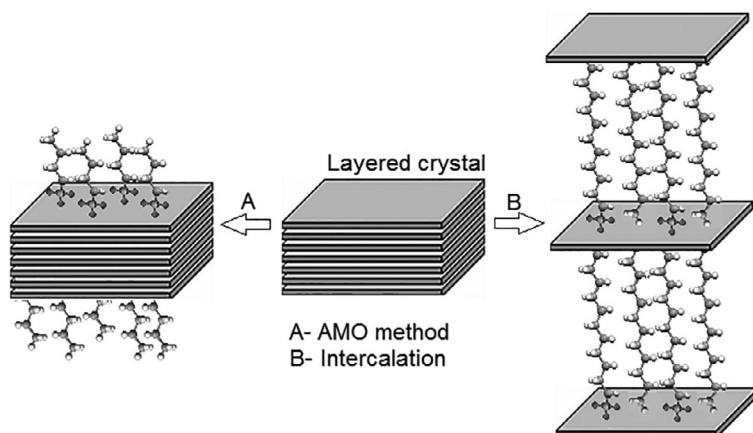

FIG. 10.13 Schematic representation of the chemical modification of a generic LDH surface.

followed by thermal decomposition of the intercalated species while maintaining the layered integrity (Baloyi et al., 2018).

These organic nanohybrid materials will not have the same thermal stability of the pillared derivatives of clay minerals, but they will have the advantage of controlling the height of the pillar by choosing the proper dicarboxylic acid and the distance between the pillars, since the exchange capacity in LDH is controlled by the $M^{2+}:M^{3+}$ molar ratio. Higher molar ratios mean fewer pillars and lower molar ratios mean more densely packed pillars, as indicated schematically in Fig. 10.14.

These new proposed porous materials will be similar to the metal organic frameworks (MOF) (Stock and Biswas, 2012; Wang and Astruc, 2020), but the pores will be allocated in a two-dimensional environment (interlayer space or gap) and potentially can be used to trap, store, and deliver several
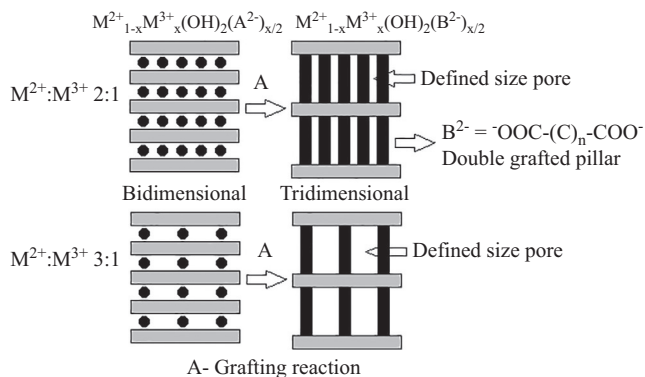
FIG. 10.14 Schematic representation of pillared layered double hydroxides by using dicarboxylates or disulfonates.

biomolecules of interest in gas storage, electrochemical energy storage and catalysis, as well as use in sensors and in filters to separate organic molecules and gases by size, since the pore sizes can be regulated as described above.

10.3 Layered hydroxide salts

Layered hydroxide salts (LHS) are described in the literature with various specific names, the most common being layered basic salts (LBS), layered basic metal salts (LBMS), metal basic salts (MBS), layered metal hydroxide salts (LMHS), and hydroxy-salts (HS). When two different metals are present in the structure of the layers, the compounds are also known as layered mixed basic salts (LMBS) or layered double hydroxide salts (LDHS) (Haan, 1963; Meyn et al., 1993; Morioka et al., 1998; Louer et al., 2001; Arizaga et al., 2007; Briois et al., 2007; Thomas, 2012).

The structures of LHS are similar to those of LDH. Despite the lower chemical diversity of the LHS, this family of compounds has greater structural diversity. The general chemical formula of an LHS is $M^{2+}(OH)_{2-x}(A^{m-})_{x/m} \cdot nH_2O$, where M^{2+} is a divalent cation, normally Mg^{2+}, Ni^{2+}, Zn^{2+}, Ca^{2+}, Cd^{2+}, Co^{2+}, or Cu^{2+}, and $(A^{m-})_{x/m} \cdot nH_2O$ is a hydrated counter-ion. In a simplified way, the basic structure of LHS can be described as derived from the structure of brucite ($Mg(OH)_2$), in which part of the structural hydroxide groups (OH^-) of the layers is replaced by water molecules or anions, and some rearrangements of the layers occur.

The most common structural examples are simonkolleite or zinc hydroxide chloride—($Zn_5(OH)_8Cl_2 \cdot H_2O$) (Allmann, 1968; Schmetzer et al., 1985; Hawthorne and Sokolova, 2002) and zinc hydroxide nitrate—($Zn_5(OH)_8 (NO_3)_2 \cdot 2H_2O$) (Stahlin and Oswald, 1970).

10.3.1 Layered hydroxides salts: Simonkolleite: $Zn_5(OH)_8Cl_2 \cdot H_2O$

In simonkolleite (Fig. 10.15), the layers are not flat as in LDH structures or in brucite, due to the presence of two distinct Zn^{2+} sites, one octahedral coordinated to six OH^- anions as in brucite $(Zn(OH)_6)$ and tetrahedral Zn^{2+} coordinated to three OH^- anions and one apical chloride anion $(Zn(OH)_3Cl)$ (Allmann, 1968; Schmetzer et al., 1985; Hawthorne and Sokolova, 2002). The octahedra share the edge and the layers are dioctahedral, similar to the structure of gibbsite, where six-member rings generate a vacant central octahedron.

Every second octahedral Zn^{2+} site is vacant, and above and below this vacant site, tetrahedral Zn^{2+} cations are positioned and water molecules are intercalated between the layers. The tridimensional structure is obtained when layers are packed across the basal axis and held together by hydrogen bonds involving intercalated water molecules, hydroxyl groups from the layers, and chloride anions grafted to the zinc top tetrahedra.

10.3.2 Layered hydroxides salts: zinc hydroxide nitrate dihydrate: $Zn_5(OH)_8(NO_3)_2 \cdot 2H_2O$

Zinc hydroxide nitrate $(Zn_5(OH)_8(NO_3)_2 \cdot 2H_2O$—or $Zn_3^{oct}Zn_2^{tet}(OH)_8$ $(NO_3)_2 \cdot 2H_2O$, where oct. and tet. represent zinc cations occupying octahedral and tetrahedral sites, respectively) (Fig. 10.16) (Stahlin and Oswald, 1970) has a similar structure as simonkolleite, with the small difference that a water molecule is coordinated directly to the tetrahedral Zn^{2+} site occupying the chloride site and the nitrate anions are intercalated between the layers, making them easy to replace by another anion and also grafted to the octahedral or tetrahedral sites (Wypych et al., 2005; Demel et al., 2011, 2014; Moyo et al., 2012; Cursino et al., 2015; Laipan et al., 2020).
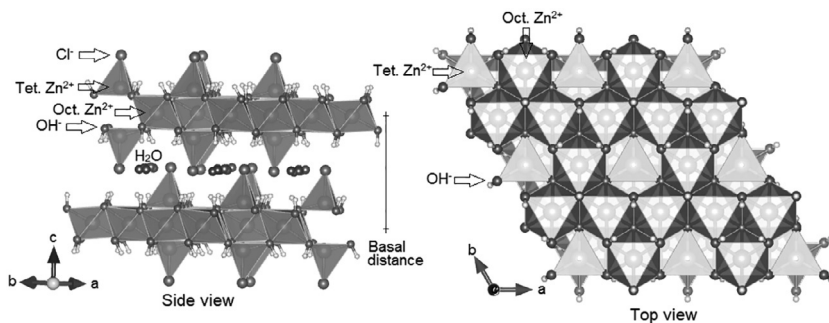

FIG. 10.15 Schematic polyhedral representation of simonkolleite's structure oriented along the indicated axis directions. Tet. Zn^{2+} represents tetrahedral sites and Oct. Zn^{2+} octahedral sites (Allmann, 1968; Schmetzer et al., 1985; Hawthorne and Sokolova, 2002).
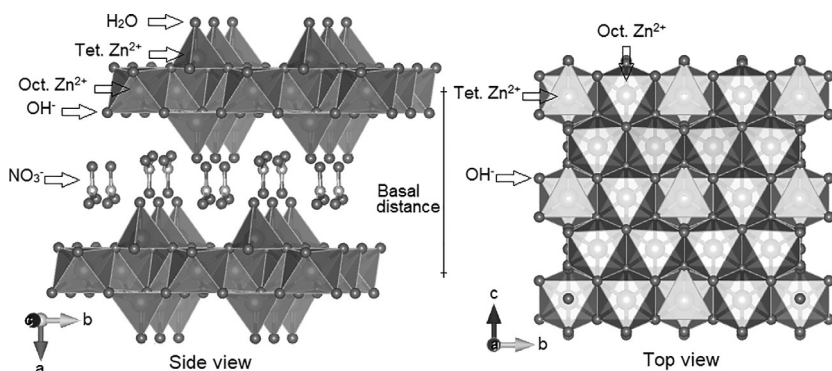
FIG. 10.16 Schematic polyhedral representation of zinc hydroxide nitrate's structure. Tet. Zn^{2+} represents tetrahedral sites and Oct. Zn^{2+} octahedral site (Stahlin and Oswald, 1970).

10.3.3 Other layered hydroxide salts

Other frequent compositions of LHS, most of them occurring in the form of minerals, are hydrozincite ($Zn_5(OH)_6(CO_3)_2$), cadmium copper hydroxide nitrate ($CdCu_3(OH)_6(NO_3)_2 \cdot H_2O$), posnjakite ($Cu_4(OH)_6SO_4 \cdot H_2O$), gerhardtite and rouaite polymorphs ($Cu_2(OH)_3NO_3$), likasite ($Cu_3(OH)_5NO_3 \cdot 2H_2O$), osakaite ($Zn_4(OH)_6SO_4 \cdot 5H_2O$), namuwite ($Zn_4(OH)_6SO_4 \cdot 4H_2O$), lahnsteinite ($Zn_4(OH)_6SO_4 \cdot 3H_2O$), anhydrous zinc hydroxide sulfate ($Zn_4(OH)_6SO_4$), anhydrous zinc hydroxide nitrate ($Zn_3(OH)_4(NO_3)_2$), botallackite ($Cu_2(OH)_3Cl$), langite ($Cu_4(OH)_6SO_4 \cdot 2H_2O$), hydrated zinc hydroxide dodecylsulfate ($Zn_5(OH)_8 (DS)_2 \cdot mH_2O$), malachite ($Cu_2(OH)_2CO_3$), nullaginite ($Ni_2(OH)_2CO_3$, pokrovskite ($Mg_2(OH)_2CO_3) \cdot 0.5 \cdot H_2O$), georgeite ($Cu_5^{2+}(OH)_4(CO_3)_3 6 \cdot H_2O$), glaukosphaerite ($(Cu,Ni)_2(OH)_2CO_3$), $Ni_2Zn_3(OH)_8(NO_3)_2 \cdot 2H_2O$, nickel-zinc hydroxide acetates ($Ni_{(3-x)}Zn_{(2+x)}(OH)_8(OAc)_2 \cdot mH_2O$), and zinc chromium hydroxide nitrate dyhydrate ($Zn_2Cr(OH)_6NO_3 \cdot 2H_2O$), etc.

10.3.4 Layered hydroxides salts: sodium-gordaite: $Zn_4(OH)_6(SO_4)$ $Cl \cdot Na(H_2O)_6$

Sodium-gordaite [$Zn_4(OH)_6(SO_4)Cl \cdot Na(H_2O)_6$] (Adiwidjaja et al., 1997; Schlüter et al., 1997; Nasdala et al., 1998) is also an interesting mineral of the LHS family, but with sui generis characteristics (Fig. 10.17).

The structure of the layers is similar to that of the mineral simonkolleite (Fig. 10.15), as well as to the structure of namuwite. As in simonkolleite, sodium-gordaite brucite-like layers present two distinct Zn^{2+} sites, one octahedral coordinated to six OH^- anions as in brucite, and tetrahedral Zn^{2+} coordinated to three OH^- anions and one apical chloride anion, as in namuwite. Above and below the vacant sites, Zn^{2+} tetrahedra are located and sulfate groups are grafted to both sides of the layers of the octahedral Zn^{+2} by replacing OH^- groups. Due to the grafting of chloride anions and sulfate anions to the
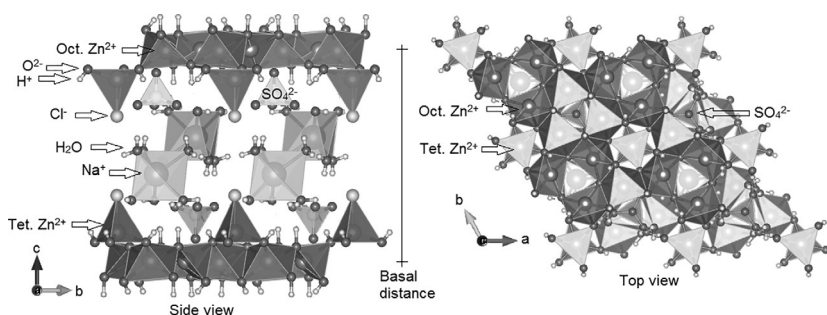
FIG. 10.17 Schematic polyhedral representation of sodium-gordaite's structure oriented along the indicated axis directions (Schlüter et al., 1977; Adiwidjaja et al., 1997; Nasdala et al., 1998).

layers, the layers are negatively charged ($[Zn_4(OH)_6(SO_4)Cl]^-$), which requires the intercalation of a cation, such as a hydrated sodium cation·($[Na(H_2O)_6]^+$).

This sui generis characteristic of having negatively charged layers is different from the other compounds of the LHS family, which have positively charged layers, so they can only exchange anions, although gordaite can exchange both cations and anions, as recently reported (Stanimirova et al., 2013; Maruyama et al., 2017; Stanimirova, 2019). In sodium gordaite, zinc cations can also be partially replaced with other cations, like Ni^{2+} and Co^{2+}, as recently reported (Kasatkin et al., 2018; Mills et al., 2019), opening even more the possibility of extending this family of compounds to other compositions.

Due to the similar structures and properties, most of the exchange reactions and chemical surface modifications of LDH have also been reported for LHS (Wypych et al., 2005; Arizaga et al., 2008), except the aqueous miscible organic (AMO) method, which has only been applied to LDH (Chen et al., 2014; Yang et al., 2014; Erastova et al., 2017). Also, ternary LHS has been described in the minerals (Oswald, 1969; Bevins et al., 1982) as well as in synthetic derivatives (Nishizawa and Yuasa, 1998; Liu et al., 2015; Oliveira and Wypych, 2016).

10.3.5 Layered hydroxides salts: Osakaite/Namuwite family: $Zn_4(OH)_6(SO_4)·nH_2O$

Zinc hydroxide sulfate occurs with variable amounts of intercalated water molecules (pentahydrated osakaite—$Zn_4(OH)_6SO_4·5H_2O$), tetrahydrated namuwite—($Zn_4(OH)_6SO_4·4H_2O$) and trihydrated lahnsteinite—($Zn_4(OH)_6SO_4·3H_2O$) as well as anhydrous form of zinc hydroxide sulfate ($Zn_4(OH)_6SO_4$), just to cite some examples (Oswald, 1969; Mellini and Merlino, 1979; Bevins et al., 1982; Bear et al., 1986; Effenberger, 1986; Groat, 1996; Chukanov et al., 2013; Germann et al., 2016; Stanimirova et al., 2017).

The schematic polyhedral representation of namuwite's structure (Fig. 10.18) (Groat, 1996) is similar to the structure of zinc hydroxide nitrate (Fig. 10.16), but instead of intercalated nitrate anions, sulfate anions are grafted on both the upper and lower layers to the octahedral zinc cations, replacing structural hydroxide anions. Since the layer is the same in the minerals cited above, the basal distances attributed to the amount of water molecules are 11.03 Å in osakaite, 10.54 Å in namuwite, 9.25 Å in lahnsteinite, and 8.93 Å in anhydrous zinc hydroxide sulfate.

10.4 Methods of synthesis

Several synthesis methods are used to prepare layered double hydroxides (LDH) and layered hydroxide salts (LHS). The most important are briefly described in this section. The majority of the examples apply to LDH, but with some adaptations, the same methods can be applied for the synthesis of LHS.

10.4.1 Coprecipitation with constant and variable pH

Coprecipitation is the main process involved in the syntheses of LDH and LHS, and the synthesis pH is normally alkaline, but is not restricted to this condition. Coprecipitation can be divided into at least three methods: constant, increasing or decreasing pH, each of which has a particular effect on the quality of the crystals, especially the sizes of the platelet-like particles and their crystallinity.

The variables that can be controlled are the pH of the final titration, concentration of the solutions, synthesis temperature, ripening time, $M^{2+}:M^{3+}$ molar ratio, stirring speed, and speed of adding chemical solutions. Even the presence of different salt anions in the solutions can influence the process and crystal quality. To obtain large well-crystallized crystals, all these synthesis parameters need to be optimized for each formulation. Ideally, a titration
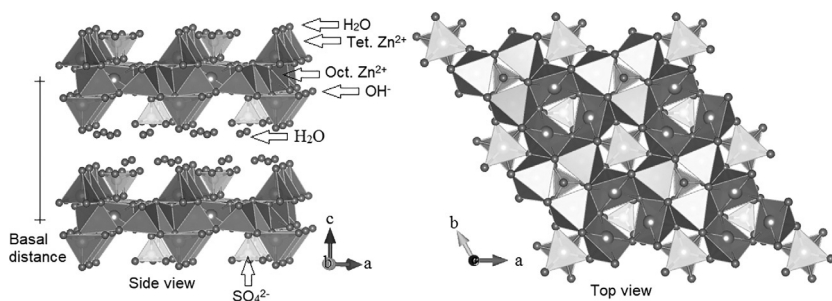

FIG. 10.18 Schematic of polyhedral representation of namuwite's structure oriented along the indicated axis directions (Groat, 1996). Tet. Zn^{2+} represents tetrahedral sites and Oct. Zn^{2+} octahedral sites.

curve needs to be constructed and the precipitation pH registered, to allow retrieving the samples at different pH levels to observe the crystallinity and the crystal quality through X-ray diffraction measurements, ideally *in situ*. To simplify the process, the solution needs to be as diluted as possible, the reaction medium should be heated and the addition needs to be very slow and under constant agitation to achieve homogenous mixture. After arriving at the desired pH, the milky dispersion in the presence of the mother solution needs to be treated at high temperature, preferably under hydrothermal conditions, for crystal ripening.

LDH and LHS are generally precipitated from a mixture of metal salts (or a single salt in the case of LHS). Normally the salts used contain the anions of interest to be intercalated. Ex.: If a LHD of Zn:Al in the molar ratio of 2:1 and intercalation with nitrate is needed, the salt solution should contain $Zn(NO_3)_2$ and $Al(NO_3)_3$ in the proportion of 2:1 and be precipitated with an alkaline solution (NaOH, KOH or NH_4OH), as indicated in Eq. (10.1).

$$2\ Zn(NO_3)_2 + Al(NO_3)_3 + 6\ NaOH \rightarrow Zn_2Al(OH)_6(NO_3) \cdot nH_2O + 6\ NaNO_3$$

(10.1)
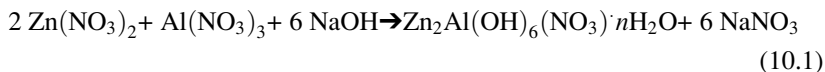
It is important to keep the concentration of the anions in excess to avoid contamination with carbonate from the CO_2 present in the air, which has strong affinity for the metal hydroxide layers, and hence has preference for intercalation in relation to nitrate. One of the reasons for this strong affinity is carbonate's double charge, while nitrate has a single charge. The higher the anion charge is, the stronger the preference for intercalation will be. Thus, to avoid intercalation of carbonate from the air, most of these reactions need to be processed under the protective atmosphere of an inert gas (normally N_2 or Ar) to exclude dissolved CO_2 from the solutions, especially from alkaline solutions. The solutions need to be prepared with decarbonated water, which is prepared by boiling distilled water with an intense flow of bubbling N_2 and must be immediately used after cooling under N_2 flow. In the case of NaOH and KOH, after opening the flask, the carbonation tends to be observed at the surface of the NaOH or KOH as a thin white layer of alkali carbonate, which also needs to be removed by washing before preparing the alkaline solutions.

After precipitation, the obtained slurry in the presence of the mother solution can be placed in a closed container and submitted hydrothermal treatment for some time (normally hours or days, depending on the temperature), to increase the particles' sizes and crystallinity (Ostwald ripening or hydrothermal crystallization). Another possibility is to keep the slurry in contact with the mother solution for some days at room temperature, or even separate the solid from the mother solution by centrifugation, immediately after precipitation. Filtering is not effective to avoid trapping soluble species in the crystal voids and adsorbed cations/anions at the particles' surfaces.

Also, to avoid any contamination, the slurry should be centrifuged, the mother solution removed, and a new portion of water should be added (normally in the same amount as present in the mother solution). The slurry is then redispersed in an ultrasound bath for some seconds. The milky dispersion should be centrifuged again, always using decarbonated water, and the process should ideally be repeated for four or five times to assure the elimination of soluble included, occluded, absorbed, and adsorbed impurities. The ideally obtained $Zn_2Al(OH)_6(NO_3) \cdot nH_2O$ can also be defined as $Zn_{0.667}Al_{0.333}$ $(OH)_2(NO_3)_{0.333} \cdot nH_2O$.

The difference among co-precipitation methods is the way the process is conducted. In the rising pH method, the pH of the mixed metal solutions, which have acid pH due to the metal hydrolysis, is slowly increased until the desired pH level with an alkaline solution, prepared normally with NaOH, KOH, or NH_4OH. The solution's concentration must be diluted (normally 0.1 mol/L or event less) and the process conducted under intense stirring to avoid supersaturation, induce crystal growth, and avoid nucleation of new crystals.

The decreasing pH method is exactly the opposite: the mixed salt solutions are added to the alkaline solution until the desired pH level is attained. Finally, in the constant pH method, both solutions (the mixed salts and the alkaline) are slowly dripped into a single recipient containing water and the pH is controlled with a pH meter, to prevent abrupt variation. Normally these methods are conducted in glass reactors where the temperature, pH, and inert atmosphere are controlled and peristaltic pumps are used to introduce the solutions in the reactor slowly.

When carbonate anions are intercalated, there is no need to control the atmosphere, and in the absence of carbonate salts, nitrate or chloride salts can be used in the presence of an excess of Na_2CO_3 to obtain the desired intercalated anions (Eq. 10.2).

$$2\,Zn(NO_3)_2 + Al(NO_3)_3 + 6\,AOH + Na_2CO_3 \rightarrow Zn_2Al(OH)_6(CO_3)_{0.5} \cdot nH_2O$$
$$+\,6\,ANO_3 + 0.5\,Na_2CO_3 + NaNO_3\ (A = Na\ or\ K)$$

$$(10.2)$$
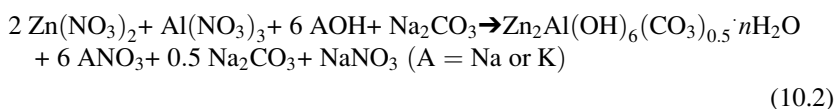
In the rising pH method care must be taken since single metal hydroxides can be precipitated at slight acid pHs (lower pHs than the precipitation of LDH or LHS) and can contaminate the samples. In this sense, solubility product constants (K_{sp}) need to be evaluated to avoid undesired contaminants, especially problematic if the hydroxides are amorphous, making them undetectable by X-ray diffraction. Also, due to the homogeneous distribution of the amorphous contaminants in the samples, even elements mapping through Energy Dispersive Spectroscopy (EDS) can indicate homogeneous distribution of the elements in the samples generating false chemical compositions.

10.4.2 Reconstruction or structural memory effect

The reconstruction or structural memory effect is normally used when a specific anion needs to be intercalated and the salts are not available (among b other reasons, like the use of nanostructured oxides in environmental remediation and catalysis). It is based on the property that LDH intercalated with carbonate can be thermally decomposed until a desired temperature is reached to promote dehydration, removal of intercalated carbonate and dehydroxylation of the layers, but not high enough to form stable crystalline oxides. The mixed oxides (normally called nanostructured mixed metal oxides (MMO) or layered double oxides—LDO) can be reconstructed to the LDH structure after hydration with water vapor or after immersing the powder in a solution containing the anions of interest (Eqs. 10.3 and 10.4).

$$Zn_2Al(OH)_6(CO_3)_{0.5} \cdot nH_2O \rightarrow 2Zn/AlO_x$$
$$+ NaCH_3COO \rightarrow Zn_2Al(OH)_6(CH_3COO) \cdot nH_2O \qquad (10.3)$$

$$Zn_2Al(OH)_6(CO_3)_{0.5} \cdot nH_2O \rightarrow 2Zn/AlO_x + water \rightarrow Zn_2Al(OH)_6(OH) \cdot nH_2O$$
$$(10.4)$$
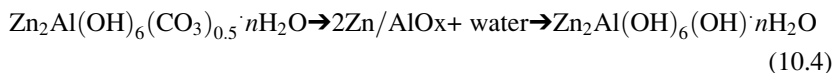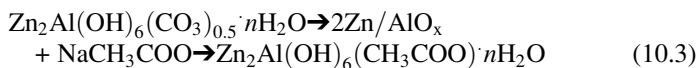
10.4.3 Mechanochemical approach

In the mechanochemical approach, the starting materials are based on the mixture of salts or oxides in the presence of a hydroxide (normally NaOH or KOH) or single hydroxides, used in the desired stoichiometric molar ratios. The mechanochemical approach was introduced to reduce the drawbacks attributed to the coprecipitation methods like the treatment of aqueous waste, high energy consumption, and complex operations during the syntheses.

   The process can occur by single-step grinding, mechano-hydrothermal, or two-step grinding (dry and wet grinding). After submitting the mixture to grinding for some time, the mixture is washed with decarbonated water, resulting in a slurry of dispersed LDH or LHS particles, similar to those obtained by co-precipitation (Eq. 10.1). This method is simple, since the process of grinding can be performed manually using a mortar and pestle (Qu et al., 2016). If carbonate is the desired intercalated anion, Na_2CO_3 can be introduced in the mixture and the reaction processed as indicated in Eq. (10.2).

10.4.4 Hydrolysis of salts and oxides

Urea hydrolysis, homogeneous precipitation or the urea method (Staal et al., 2017) is the preferred method for the preparation of pure and highly crystalline layered double hydroxides. This method is based on the thermal decomposition of excess urea in water (Eqs. 10.5–10.7), in the presence of an acidic solution of salts (or even a single metal salt), to generate hydroxide anions

homogeneously in the solution and precipitate highly crystalline carbonate intercalated layered hydroxides with large particles.

$$(NH_2)_2CO + H_2O + heat \rightarrow 2\ NH_3 + CO_2 \tag{10.5}$$
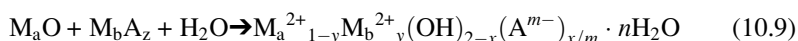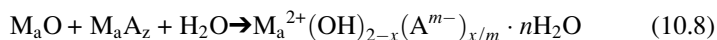
$$CO_2 + H_2O \rightarrow H_2CO_3 \leftrightharpoons 2H^+ + CO_3^{2-} \tag{10.6}$$

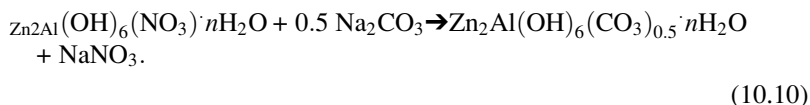$$NH_3 + H_2O \leftrightharpoons NH_4OH \leftrightharpoons NH_4^+ + OH^- \tag{10.7}$$
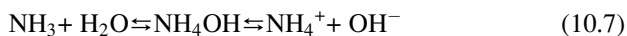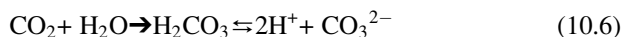
Despite the large number of publications reporting this method, recently (Staal et al., 2017), it was observed that amorphous mixtures of single hydroxides can contaminate the samples and less than half of the total Al^{3+} content was incorporated in ZnAl-LDH, especially with specific $M^{2+}:M^{3+}$ molar ratios, giving a false impression that LDH are pure. So, this method should be used carefully to avoid these problems.

Still using the hydrolysis approach, used more frequently for the synthesis of LHS, trivalent metal salts like $AlCl_3$ and $CrCl_3$ can be hydrolyzed in the presence of insoluble divalent metal oxides like ZnO, NiO, and CuO, producing an LHS with the composition $M^{2+}(OH)_{2-x}(A^{m-})_{x/m} \cdot nH_2O$ (Eq. 10.8). The same method can be used to produce layered double hydroxide salts (LDHS) with the composition $M_a^{2+}{}_{1-y}M_b^{2+}{}_y(OH)_{2-x}(A^{m-})_{x/m} \cdot nH_2O$, where M_a and M_b are two different divalent metal cations, such as Co, Ni, Zn, etc., as indicated in Eq. (10.9) (Arizaga et al., 2007).

$$M_aO + M_aA_z + H_2O \rightarrow M_a^{2+}(OH)_{2-x}(A^{m-})_{x/m} \cdot nH_2O \tag{10.8}$$

$$M_aO + M_bA_z + H_2O \rightarrow M_a^{2+}{}_{1-y}M_b^{2+}{}_y(OH)_{2-x}(A^{m-})_{x/m} \cdot nH_2O \tag{10.9}$$

10.4.5 Exchange reactions

The exchange method to produce new LDS and LHS is extensively used and the reactions are normally topotactic. This method is simple and consists of synthesizing a LDH or LHS by the conventional method and replacing the intercalated anions by dispersion of the solid in a solution containing the anions of interest (Biswick et al., 2006). Chloride and nitrate are frequently used for exchange, since these anions are easily exchangeable with other anions. The process was already schematically represented in Figs. 10.3–10.6 (Eq. 10.10).

$$\begin{aligned} &_{Zn2Al}(OH)_6(NO_3) \cdot nH_2O + 0.5\ Na_2CO_3 \rightarrow Zn_2Al(OH)_6(CO_3)_{0.5} \cdot nH_2O \\ &+ NaNO_3. \end{aligned}$$

$$\tag{10.10}$$

In the case of a need for a well-crystallized sample and bigger crystal sizes, intercalation with carbonate can be used (most of the time prepared by urea hydrolysis). But since carbonate is strongly bonded to the layers, this process can only occur by treating the LDH-CO$_3$ phase with a buffer solution

of NaCl/NaCH$_3$COOH/CH$_3$COOH (Iyi and Sasaki, 2008; Hibino, 2014) at slightly acidic pH. The protons react with the interlayer carbonate ions to form bicarbonate and finally carbonic acid, which will be decomposed to CO$_2$ and water and released as gas from the sample. Chloride anions from NaCl, used in excess in the buffer solution, will then replace the intercalated carbonate (Eq. 10.11). This reaction will not occur if the LDH-CO$_3$ phase is treated directly with NaCl solution. Also, severe damage to the layers must be avoided by careful pH control through the use of the buffer solution.

$$Zn_2Al(OH)_6(CO_3)_{0.5} \cdot nH_2O + NaCl + NaCH_3COO$$
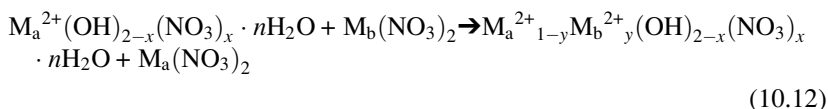$$+ CH_3COOH \rightarrow Zn_2Al(OH)_6(Cl) \cdot nH_2O + CO_2 + H_2O \qquad (10.11)$$
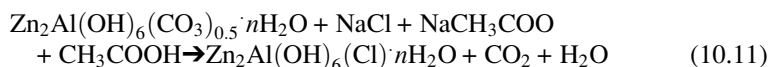
10.4.6 Diadochy reactions

Diadochy reactions are one of the rarest possibilities of isomorphic substitution of metal cations located in the main hydroxide layers (interlayer domain) in a previously synthesized material, allocated in octahedral or tetrahedral sites by other metal cations with the same oxidation state (Komarneni et al., 1998). This process is frequently applied to LHS with the composition $M_a^{2+}(OH)_{2-x}(A^{m-})_{x/m} \cdot nH_2O$, which after the reaction is transformed to $M_a^{2+}{}_{1-y}M_b^{2+}{}_y(OH)_{2-x}(A^{m-})_{x/m} \cdot nH_2O$ (Eq. 10.12) (M_a and M_b are two different divalent metal cations).

$$M_a^{2+}(OH)_{2-x}(NO_3)_x \cdot nH_2O + M_b(NO_3)_2 \rightarrow M_a^{2+}{}_{1-y}M_b^{2+}{}_y(OH)_{2-x}(NO_3)_x$$
$$\cdot nH_2O + M_a(NO_3)_2$$

$$(10.12)$$

In the case of LHS involving Zn, an interesting example is the compound [$Zn_3^{oct}Zn_2^{tet}(OH)_8(CH_3COO)_2 \cdot 2H_2O$], where three zinc cations are allocated in octahedral sites (oct) and two zinc cations are allocated in tetrahedral sites (tet), as in $Zn_5(OH)_8(NO_3)_2 \cdot 2H_2O$ (Fig. 10.16). When these compounds are put in contact with solutions of nickel salts, Ni^{2+} can selectively replace the Zn^{2+} allocated in the octahedral sites, obtaining $Ni_3^{oct}Zn_2^{tet}(OH)_8(CH_3COO)_2 \cdot 2H_2O$. The same composition is used to obtain mixed $2Zn^{2+}/3Ni^{2+}$ salts by direct precipitation from the salts in solution (Nishizawa and Yuasa, 1998; Tessier et al., 2000; Kolinjavadi et al., 2019).

10.4.7 Sol/gel method

In the sol-gel method, normally the organic salts, like alkoxides and acetyla-cetonates, of the LDH metal components that need to be obtained are dissolved in an organic solvent, typically ethanol or acetone, and the pH is adjusted with NH$_4$OH. The gel obtained is refluxed for the complete metal-organic metal hydrolysis and isolated by filtration, and then washed and dried (Aranmedia et al., 2002). Due to the better homogeneity of the

dissolved metal-organic metal salts, this route is normally applied to prepare mixtures of metal oxides used in catalysis after calcination, which results in materials with more uniform pore sizes and higher surface area in comparison with the LDH obtained by co-precipitation (Prince et al., 2009). After drying the sol-gel, porous monoliths can also be obtained, which have high porosity and can be used to immobilize biological molecules like enzymes to be used in enzymatic catalysis.

Other less frequently used methods are the precipitation using organic solvents, the electrochemical synthesis, microwave–assisted precipitation, etc.

10.5 Some applications and future perspectives

There are many potential uses of natural and synthetic layered double hydroxides and hydroxide salts, such as drug delivery (Wei et al., 2005; Cao et al., 2020), energy conversion and storage (Chen et al., 2020), environmental remediation (Chaillot et al., 2021), catalysis (Stamate et al., 2020), analytical chemistry applications (Tang et al., 2020), photocatalysis (Yang et al., 2020; Zhang et al., 2020), production of sensors (Khenifi et al., 2009; Baig and Sajid, 2017), flame retardants and smoke suppressors (Ling et al., 2005; Shi et al., 2005; Matusinovic and Wilkie, 2012; Gao et al., 2014), nanocontainers to prevent corrosion of metallic surfaces (Zhang et al., 2008; Leal et al., 2020), functional polymer nanocomposites (Marangoni et al., 2009; Silva et al., 2012; Zimmermann et al., 2013; Gomez et al., 2020; Mochane et al., 2020), concrete hardening accelerators (Xu et al., 2009; Mir et al., 2020), magneto-optical devices (Liu et al., 2006), slow-release fertilizers, pesticides and herbicides (Everaert et al., 2016), Pickering emulsions (Machado et al., 2019; Amaral et al., 2020), antimicrobial, antibacterial, and antifungal substances (Ryu et al., 2010; Yang et al., 2013; Li et al., 2019; Mishra et al., 2019), electrocatalysis of water splitting, which involves hydrogen evolution (HER) and oxygen evolution reactions (OER) (Song and Hu, 2014; Yan et al., 2016; Wang et al., 2018), separation of mixtures of isomers by selective intercalation (Williams et al., 2006b), simonkolleite deposited on nickel foam/graphene for electrochemical supercapacitors (Khamlich et al., 2013), among others.

The exfoliation of sodium-gordaite and other layered hydroxide salts was recently studied by DFT under periodic boundary conditions with plane wave functions as a basis set (Tavares et al., 2019). Interesting exfoliation energies and changes in electrical properties were found, which opens possibilities for further experimental investigations.

The number of LDH and LHS possible combinations of metals and intercalated anions is almost unlimited and still a lot of work needs to be done in the synthesis of new compounds with different compositions, explore the morphologies and in spite of that broad range of applications, new opportunities are still to be discovered, especially for LHS, which have been investigated less. They have structural diversity and strong potential to generate

important applications. The class of layered compounds is very important due to the unique structure, which can be delaminated/exfoliated to obtain materials with new and exotic properties due to the quantum effects at nanoscale. Delaminated and exfoliated materials consist basically of surfaces and functionalization can also attribute new properties in particles dispersions or after restacking. Devices can also be imagined after evaporating exfoliated dispersions in the form of thin films.

The grafting of carboxylate groups in the layers of LHS (Newman and Jones, 1999), pillaring of cobalt LHS with diamines ($Co_4(SO_4)(OH)_6(H_2NC_2H_4NH_2)_{0.5} \cdot 3H_2O$) (Rujiwatra et al., 1999), and pillaring of materials with dicarboxylates or disulfonates are also expected to produce novel materials similar to the pillared clay minerals (PILC). The synthesis and investigation of the properties of these new materials with extremely high surface area, varied chemical functionalities in the pillars, and structural variability are promising in several branches of science and technology.

The tuneable nature of the LDH which results from the range of methods of synthesis, variable combination of metal cations in the layers, and the broad range of intercalated anionic species still needs to be understood to expose the full potential of this class of compounds.

We hope this chapter has provided ideas to readers about the structure, properties, and challenges still to overcome and opportunities to develop materials with new and unique properties based on this fascinating class of compounds.

Acknowledgments

References

Adachi-Pagano, M., Forano, C., Besse, J.P., 2000. Delamination of layered double hydroxides by use of surfactants. Chem. Commun. 1, 91–92.

Adiwidjaja, G., Friese, K., Klaska, K.H., Schluter, J., 1997. The crystal structure of gordaite NaZn$_4$(SO$_4$)(OH)$_6$Cl.6H$_2$O. Zeitsch. Kristallogr. 212, 704–707.

Agakhanov, A.A., Karpenko, V.Y., Pautov, L.A., Uvarova, Y.A., Sokolova, E., Hawthorne, F.C., Bekenova, G.K., 2005. Kyrgyzstanite, ZnAl$_4$(SO$_4$)(OH)$_{12}$·3H$_2$O, A new mineral from the Kara-Tangi deposit, Kirgizia. New data on Miner. 40, 23–28.

Ahmed, I.A.M., Benning, L.G., Kakonyi, G., Sumoondur, A.D., Terrill, N.J., Shaw, S., 2010. Formation of green rust sulfate: a combined in situ time-resolved X-ray scattering and electrochemical study. Langmuir 26, 6593–6603.

Allmann, R., 1968. Verfeinerung der struktur des zinkhydroxidchlorids II, $Zn_5(OH)_8Cl_2$. $1H_2O$. Zeitsch. Kristallogr. 126 (5–6), 417–426.

Amaral, L.F.M., de Freitas, R.A., Wypych, F., 2020. K-shigaite-like layered double hydroxide particles as Pickering emulsifiers in oil/water emulsions. Appl. Clay Sci. 193, 105660.

Arakcheeva, A.V., Pushcharovsky, D.Y., Rastsvetaeva, R.K., Atencio, D., Lubman, G.U., 1996. Crystal structure and comparative crystal chemistry of $Al_2Mg_4(OH)_{12}(CO_3)\cdot 3H_2O$, a new mineral from the hydrotalcite-manasseite group. Crystallogr. Rep. 41, 972–979.

Aranmedia, M.A., Borau, V., Jimenez, C., Marinas, J.M., Ruiz, J.R., Urbano, F.J., 2002. Comparative study of Mg/M(III) (M=Al, Ga, In) layered double hydroxides obtained by coprecipitation and the sol/gel method. J. Solid State Chem. 168, 156–161.

Arizaga, G.G.C., Mangrich, A.S., Gardolinski, J.E.F.C., Wypych, F., 2008. Chemical modification of zinc hydroxide nitrate and Zn-Al-layered double hydroxide with dicarboxylic acids. J. Colloid Interface Sci. 320 (1), 168–176.

Arizaga, G.G.C., Satyanarayana, K.G., Wypych, F., 2007. Layered hydroxide salts: synthesis, properties and potential applications. Solid State Ion. 178, 1143–1162.

Baig, N., Sajid, M., 2017. Applications of layered double hydroxides based electrochemical sensors for determination of environmental pollutants: a review. Trends Environ. Anal. Chem. 16, 1–15.

Baloyi, J., Ntho, T., Moma, J., 2018. Synthesis and application of pillared clay heterogeneous catalysts for wastewater treatment: a review. RSC Adv. 8, 5197–5211.

Bear, I.J., Grey, I.E., Madsen, I.C., Newnham, I.E., Rogers, L.J., 1986. Structures of the basic zinc sulfates $3Zn(OH)_2.ZnSO_4.mH_2O$, m = 3 and 5. Acta Crystallogr. B 42, 32–39.

Besserguenev, A.V., Fogg, A.M., Francis, R.J., Price, S.J., O'Hare, D., Isupov, V.P., Tolochko, B.P., 1997. Synthesis and structure of the gibbsite intercalation compounds $[LiAl_2(OH)_6]X$ {X = Cl, Br, NO_3} and $[LiAl_2(OH)_6]Cl\cdot H_2O$ using synchrotron X-ray and neutron powder diffraction. Chem. Mater. 9, 241–247.

Bevins, R.E., Turgoose, S., Williams, P.A., 1982. Namuwite, $(Zn,Cu)_4SO_4(OH)_6\cdot 4H_2O$, a new mineral from Wales. Mineral. Mag. 46, 51–54.

Biswick, T., Jones, W., Pacula, A., Serwicka, E., 2006. Synthesis, characterisation and anion exchange properties of copper, magnesium, zinc and nickel hydroxy nitrates. J. Solid State Chem. 179 (1), 49–55.

Booking, A.S., Drits, V.A., 1993. Polytype diversity of the hydrotalcite-like minerals. I. Possible polytypes and their diffraction features. Clays Clay Miner. 41 (5), 551–557.

Briois, V., Giorgetti, C., Baudelet, F., Blanchandin, S., Tokumoto, M.S., Pulcinelli, S.H., Santilli, C.V., 2007. Dynamical study of ZnO nanocrystal and Zn-HDS layered basic zinc acetate formation from sol-gel route. J. Phys. Chem. C 111, 3253–3258.

Britto, S., Kamath, P.V., 2014. Synthesis, structure refinement and chromate sorption characteristics of an Al-rich bayerite-based layered double hydroxide. Solid State Chem. 215, 206–210.

Bubniak, G.A., Schreiner, W.H., Mattoso, N., Wypych, F., 2002. Preparation of a new nanocomposite of $Al_{0.33}Mg_{0.67}(OH)_2(C_{12}H_{25}SO_4)_{0.33}$ and poly(ethylene oxide). Langmuir 18, 5967–5970.

Cao, Z., Li, B., Sun, L., Li, L., Ping, Z., Gu, Z., 2020. Targeted drug delivery: 2D layered double hydroxide nanoparticles: recent progress toward preclinical/clinical nanomedicine. Small 4 (2), 2070008.

Carlino, S., 1997. The intercalation of carboxylic acids into layered double hydroxides: a critical evaluation and review of the different methods. Solid State Ion. 98, 73–84.

Chaillot, D., Bennici, S., Brendle, J., 2021. Layered double hydroxides and LDH-derived materials in chosen environmental applications: a review. Environ. Sci. Pollut. Res. Int. 28, 24375–24405. https://doi.org/10.1007/s11356-020-08498-6.

Chen, C., Tao, L., Du, S., Chen, W., Wang, Y., Zou, Y., Wang, S., 2020. Advanced exfoliation strategies for layered double hydroxides and applications in energy conversion and storage. Adv. Fuct. Mater. 30 (14), 1909832.

Chen, C., Yang, M., Wang, Q., Buffet, J.C., O'Hare, D., 2014. Synthesis and characterisation of aqueous miscible organic-layered double hydroxides. J. Mater. Chem. A 2 (36), 15102–15110.

Christiansen, B.C., Balic-Zunic, T., Petit, P.O., Frandsen, C., Mørup, S., Geckeis, H., Katerinopoulou, A., Stipp, S.L.S., 2009. Composition and structure of an iron-bearing, layered double hydroxide (LDH)—green rust sodium sulphate. Geochim. Cosmochim. Acta 73, 3579–3592.

Christiansen, B.C., Dideriksen, K., Katz, A., Nedel, S., Bovet, N., Sørensen, H.O., Frandsen, C., Gundlach, C., Andersson, M.P., Stipp, S.L.S., 2014. Incorporation of monovalent cations in sulfate green rust. Inorg. Chem. 53, 8887–8894.

Chukanov, N.V., Rastsvetaeva, R.K., Aksenov, S.M., Pekov, I.V., Belakovsky, D.I., Blass, G., Möhn, G., 2013. Lahnsteinite, $Zn_4(SO_4)(OH)_6 \cdot 3H_2O$, a new mineral from the Friedrichssegen mine Germany. Geol. Ore Deposits 55, 663–668.

Clark, G.R., Rodgers, A., Herderson, G.S., 1998. The crystal chemistry of doyleite, $Al(OH)_3$. Zeitsch. Kristallogr. 213, 96–100.

Clearfield, A., Kieke, M., Kwan, J., Colon, J.L., Wang, R.C., 1991. Intercalation of dodecyl sulfate into layered double hydroxides. J. Inclus. Phen. Mol. Recog. Chem. 11, 361–378.

Constantino, V.R.L., Pinnavaia, T.J., 1995. Basic Properties of $Mg_{1-x}^{2+}Al_x^{3+}$ layered double hydroxides intercalated by carbonate, hydroxide, chloride, and sulfate anions. Inorg. Chem. 34, 883–892.

Cooper, M.A., Hawthorne, F.C., 1996. The crystal structure of Shigaite, $[AlMn_2^{2+}(OH)_6]_3(SO_4)_2$. $Na(H_2O)_6(H_2O)_6$, a hydrotalcite-group mineral. Can. Mineral. 34, 91–97.

Crepaldi, E.L., Pavan, P.C., Valim, J.B., 1999. A new method of intercalation by anion exchange in layered double hydroxides. Chem. Commun. 2, 155–156.

Cursino, A.C.T., Lisboa, F.S., Pyrrho, A.S., Souza, V.P., Wypych, F., 2013. Layered double hydroxides intercalated with anionic surfactants/benzophenone as potential materials for sunscreens. J. Colloid Interface Sci. 397, 88–95.

Cursino, A.C.T., Rives, V., Carlos, L.D., Rocha, J., Wypych, F., 2015. Layered zinc hydroxide salts intercalated with anionic surfactants and adsolubilized with UV absorbing organic molecules. J. Braz. Chem. Soc. 26 (9), 1769–1780.

Demel, J., Hynek, J., Kovar, P., Dai, Y., Taviot-Gueho, C., Demel, O., Pospisil, M., Lang, K., 2014. Insight into the structure of layered zinc hydroxide salts intercalated with dodecyl sulfate anions. J. Phys. Chem. C 118 (46), 27131–27141.

Demel, J., Plestil, J., Bezdicka, P., Janda, P., Klementova, M., Lang, K., 2011. Layered zinc hydroxide salts: Delamination, preferred orientation of hydroxide lamellae, and formation of ZnO nanodiscs. J. Colloid Interface Sci. 360 (2), 532–539.

Duan, X., Evans, D.G. (Eds.), 2006. Layered Double Hydroxides. Springer.

Effenberger, H., 1986. Likasite, $Cu_3(OH)_5(NO_3) \cdot 2H_2O$: revision of the chemical formula and redetermination of the crystal structure. Neues Jahrb. Mineral. Monatsh., 101–110.

Erastova, V., Degiacomi, M.T., O'Hare, D., Greenwell, H.C., 2017. Understanding surface interactions in aqueous miscible organic solvent treated layered double hydroxides. RSC Adv. 7, 5076–5083.

Everaert, M., Warrinnier, R., Baken, S., Gustafsson, J.P., 2016. Phosphate-exchanged Mg-Al layered double hydroxides: a new slow release phosphate fertilizer. ACS Sust. Chem. Eng. 4 (8), 4280–4287.

Feitknecht, W., Gerber, M., 1942. Zur kenntnis der doppelhydroxyde und basischen doppelsalze III. Über magnesium-aluminiumdoppelhydroxyd. Helv. Chim. Acta 25, 131–137.

Fogg, A.M., Williams, G.R., Chestera, R., O'Hare, D., 2004. A novel family of layered double hydroxides—[MAl$_4$(OH)$_{12}$](NO$_3$)$_2$·xH$_2$O (M = Co, Ni, Cu, Zn). J. Mater. Chem. 14, 2369–2371.

Gao, Y., Wu, J., Wang, Q., Wilkie, C.A., O'Hare, D., 2014. Flame retardant polymer/layered double hydroxide nanocomposites. J. Mater. Chem. A 2, 10996–11016.

Germann, L.S., Dinnebier, R.E., Liu, X., Dong, Y., Li, W., 2016. On the crystal structure of a previously unknown anhydrous zinc hydroxide sulfate. Z. Anorg. Allg. Chem. 642, 255–259.

Gomez, N.A.G., Maruyama, S.A., Leuteritz, A., Wypych, F., 2020. Composites of polyethylene and layered cobalt hydroxide salts as potential ultraviolet radiation absorbers. Polym. Bull. 77, 255–273.

Groat, L.A., 1996. The crystal structure of namuwite, a mineral with Zn in tetrahedral and octahedral coordination, and its relationship to the synthetic basic zinc sulfates. Am. Mineral. 81, 238–243.

Guimarães, J.L., Marangoni, R., Ramos, L.P., Wypych, F., 2000. Covalent grafting of ethylene glycol into the Zn-Al-CO$_3$ layered double hydroxide. J. Collloid Interface Sci. 227, 445–451.

Guinier, A., Bokij, G.B., Boll-Dornberger, K., Cowley, J.M., Durovic, S., Jagodzinski, H., Krishna, P., Wolff, P.M., Zvyagin, B.B., Cox, D.E., Goodman, P., Hahn, T., Kuchitsu, K., Abrahams, S.C., 1984. Nomenclature of polytype structures. Acta Crystallogr. A 40, 399–404.

Guo, X.X., Zhang, F.Z., Evans, D.G., Duan, X., 2010. Layered double hydroxide films: synthesis, properties and applications. Chem. Commun. 46, 5197–5210.

Haan, Y.M., 1963. Interdiffusion method for the preparation of single crystals of certain hydroxides and basic salts. Nature 200, 876.

Hawthorne, F.C., Cooper, M.A., 2013. The crystal structure of chalcoalumite: mechanisms of Jahn-Teller-driven distortion in [6]Cu^{2+}-containing oxysalts. Miner. Mag. 77, 2901–2912.

Hawthorne, F.C., Sokolova, E., 2002. Simonkolleite, Zn$_5$(OH)$_8$Cl$_2$ H$_2$O, A decorated interrupted-sheet structure of the form [M phi (2)](4). Can. Mineral. 40, 939–946.

Hermans, J.J., Keune, K., Loon, A.V., Corkery, R.W., Iedema, P.D., 2014. The molecular structure of three types of long-chain zinc(II) alkanoates for the study of oil paint degradation. Polyhedron 81, 335–340.

Hibino, T., 2014. Acid treatment of layered double hydroxides containing carbonate. Eur. J. Inorg. Chem. 31, 5311–5321.

Song, F., Hu, X., 2014. Exfoliation of layered double hydroxides for enhanced oxygen evolution catalysis. Nat. Commun. 5, 4477.

Huminicki, D.M.C., Hawthorne, F.C., 2003. The crystal structure of Nikischerite, NaFe$_6^{2+}$ Al$_3$(SO$_4$)$_2$.(OH)$_{18}$.(H$_2$O)$_{12}$, a mineral of the Shigaite group. Can. Mineral. 41, 79–82.

Iyi, N., Sasaki, T., 2008. Decarbonation of MgAl-LDHs (layered double hydroxides) using acetate-buffer/NaCl mixed solution. J. Colloid Interface Sci. 322 (1), 237–245.

Jensen, N.D., Duong, N.T., Bolanz, R., Nishiyama, Y., Rasmussen, C.A., Gottlicher, J., Steininger, R., Prevot, V., Nielsen, U.G., 2019. Synthesis and structural characterization of a pure ZnAl$_4$(OH)$_{12}$(SO$_4$)$_2$6H$_2$O layered double hydroxide. Inorg. Chem. 58, 6114–6122.

Kameda, T., Yamazaki, T., Yoshioka, T., 2008. Preparation and characterization of Mg–Al layered double hydroxides intercalated with benzenesulfonate and benzenedisulfonate. Microp. Mesop. Mater. 114 (1–3), 410–415.

Karpenko, V.Y., Zhitova, E.S., Pautov, L.A., Agakhanov, A.A., Siidra, O.I., Krzhizhanovskaya, M.G., Rassulov, V.A., Bocharov, V.N., 2020. Akopovaite,

Li$_2$Al$_4$(OH)$_{12}$(CO$_3$)(H$_2$O)$_3$, a new Li member of the hydrotalcite supergroup from Turkestan Range, Kyrgyzstan. Miner. Mag. 84 (2), 301–311.

Kasatkin, A.V., Plášil, J., Škoda, R., Belakovskiy, D.I., Marty, J., Meisser, N., Pekov, I.V., 2018. Redefinition of thérèsemagnanite, NaCo$_4$(SO$_4$)(OH)$_6$Cl·6H$_2$O: new data and relationship to 'cobaltogordaite'. Miner. Mag. 82, 159–170.

Khamlich, S., Bello, A., Fabiane, M., Ngom, B.D., Manyala, N., 2013. Hydrothermal synthesis of simonkolleite microplatelets on nickel foam-graphene for electrochemical supercapacitores. J. Solid State Chem. 17, 2879–2886.

Khenifi, A., Derriche, Z., Forano, C., Prevot, V., Mousty, C., Scavetta, E., Ballarin, B., Guadagnini, L., Tonelli, D., 2009. Glyphosate and glufosinate detection at electrogenerated NiAl-LDH thin films. Anal. Chim. Acta 654, 97–102.

Kolinjavadi, M.R., Bhojaraj, Rajamathi, M., 2019. Nickel-zinc hydroxy salts with varying amounts of octahedral Zn^{2+}: trends in stability and selectivity in anion exchange reaction. J. Chem. Sci. 31, 112.

Komarneni, S., Kozai, N., Roy, R., 1998. Novel function for anionic clays: selective transition metal cation uptake by diadochy. J. Mater. Chem. 8, 1329–1331.

Kühl, S., Kasatkin, I., Hävecker, M., Schlögl, R., Behrens, M., 2015. Ternary and quaternary Cr or Ga-containing ex-LDH catalysts - Influence of the additional oxides onto the microstructure and activity of Cu/ZnAl$_2$O$_4$ catalysts. Catal. Today 246, 92–100.

Laipan, M., Yu, J., Zhu, R., Zhu, J., Smith, A.T., He, H., O'Hare, D., Sun, L., 2020. Functionalized layered double hydroxides for innovative applications. Mater. Horiz. 7, 715–745.

Leal, D.A., Wypych, F., Marino, C.E.B., 2020. Zinc-layered hydroxide salt intercalated with molybdate anions as a new smart nanocontainer for active corrosion protection of carbon steel. ACS Appl. Mater. Interfaces 12 (17), 19823–19833.

Lei, X., Wang, L., Zhao, X., Chang, Z., Jiang, M., Yan, D., Sun, X., 2013. Oriented CuZnAl ternary layered double hydroxide films: in situ hydrothermal growth and anticorrosion properties. Ind. Eng. Chem. Res. 52 (50), 17934–17940.

Li, M., Sultanbawa, Y., Xu, Z.P., Gu, W., Chen, W., Liu, J., Qian, G., 2019. High and long-term antibacterial activity against Escherichia coli via synergy between the antibiotic penicillin G and its carrier ZnAl layered double hydroxide. Colloids Surf. B Biointerfaces 1 (174), 435–442.

Ling, S., Li, D.Q., Li, S., Wang, J., D.G.E, Duan, X., 2005. The structure, flame retarding and smoke suppressing properties of Zn-Mg-Al-CO$_3^{2-}$ layered double hydroxides. Chin. Sci. Bull. 50, 1101–1104.

Liu, Z., Ma, R., Osada, M., Iyi, N., Ebina, Y., Takada, K., Sasaki, T., 2006. Synthesis, anion exchange, and delamination of Co-Al layered double hydroxide: assembly of the exfoliated nanosheet/polyanion composite films and magneto-optical studies. J. Am. Chem. Soc. 128, 4872–4880.

Liu, J.X., Wang, J.L., Zhang, X.G., Fang, B.B., Hu, P., Zhao, X.Y., 2015. Preparation and structural characterization of zwitterionic surfactant intercalated into NiZn-layered hydroxide salts. J. Phys. Chem. Solid 85, 180–187.

Louer, D., Rius, J., Bénard-Rocherullé, P., Louer, M., 2001. Structural study of cadmium hydroxide sulfates. VI. The layer structure of Cd$_4$SO$_4$(OH)$_6$1.5H$_2$O studied from X-ray powder and single-crystal diffraction data. Powder Diffr. 16, 86–91.

Machado, J.P.E., de Freitas, R.A., Wypych, F., 2019. Layered clay minerals, synthetic layered double hydroxides and hydroxide salts applied as Pickering emulsifiers. Appl. Clay Sci. 169, 10–20.

Marangoni, R., Ramos, L.P., Wypych, F., 2009. New multifunctional materials obtained by the intercalation of anionic dyes into layered zinc hydroxide nitrate followed by dispersion into poly(vinyl alcohol) (PVA). J. Colloid Interface Sci. 330, 303–309.

Maruyama, S.A., Krause, F., Tavares Filho, S.R., Leitão, A.A., Wypych, F., 2017. Synthesis, cation exchange and dehydration/rehydration of sodium gordaite: $NaZn_4(OH)_6(SO_4)Cl \cdot 6H_2O$. Appl. Clay Sci. 146, 100–105.

Matusinovic, Z., Wilkie, C.A., 2012. Fire retardancy and morphology of layered double hydroxide nanocomposites: a review. J. Mater. Chem. 22, 18701–18704.

Mellini, M., Merlino, S., 1979. Posnjakite $\overset{2}{\infty}$ ($Cu_4(OH)_6(H_2O)SO_4$) octahedral sheets in its structure. Locality: Fowey Consols, England. Zeitsch. Kristallogr. 149, 249–259.

Meyn, M., Beneke, K., Lagaly, G., 1993. Anion-exchange reactions of hydroxy double salts. Inorg. Chem. 32 (7), 1209–1215.

Mills, S.J., Christy, A.G., Genin, J.M.R., Kameda, T., Colombo, F., 2012a. Nomenclature of the hydrotalcite supergroup: natural layered double hydroxides. Miner. Mag. 76 (5), 1289–1336.

Mills, S.J., Christy, A.G., Kampf, A.R., Hourley, R.M., Favreau, G., Boulliard, J.C., Bourgoin, V., 2012b. Zincalstibite-9R: the first nine-layer polytype with the layered double hydroxide structure-type. Miner. Mag. 76 (5), 1337–1345.

Mills, S.J., Missen, O.P., Favreau, G., 2019. The crystal structure of Ni-rich gordaiteThérèsemagnanite from Cap Garonne. France. Miner. Mag. 83, 459–463.

Mir, Z.M., Bastos, A., Hoche, D., Zheludkevich, M.L., 2020. Recent advances on the application of layered double hydroxides in concrete—a review. Mater. 13 (6), 1426.

Mishra, G., Dash, B., Pandey, S., Sethi, D., Kumar, C.G., 2019. Comparative evaluation of synthetic routes and antibacterial/antifungal properties of Zn-Al layered double hydroxides containing benzoate anion. Environ. Eng. Sci. 35, 3.

Miyata, S., 1983. Anion-exchange properties of hydrotal-cite-like compounds. Clays Clay Miner. 31, 305–311.

Mochane, M.J., Magagula, S.I., Sefadi, J.S., Sadiku, E.R., Mokhena, T.C., 2020. Morphology, thermal stability, and flammability properties of polymer- layered double hydroxides (LDH) nanocomposites: a review. Crystals 10 (7), 612.

Momma, K., Izumi, F., 2011. VESTA 3 for three-dimensional visualization of crystal, volumetric and morphology data. J. Appl. Cryst. 44, 1272–1276.

Morioka, H., Tagaya, H., Karasu, M., Kadokawa, J.I., Chiba, K., 1998. Preparation of hydroxy double salts exchanged by organic compounds. J. Mater. Res. 13, 848–851.

Moyo, L., Focke, W., Labuschagne, J., Verryn, S., 2012. Layered double hydroxide intercalated with sodium dodecyl sulfate. Mol. Cryst. Liquid Cryst. 555, 51–64.

Nasdala, L., Witzke, T., Ullrich, B., Brett, R., 1998. Gordaite [$Zn_4Na(OH)_6(SO_4)Cl \cdot 6H_2O$]: second occurrence in the Juan de Fuca Ridge, and new data. Am. Mineral. 83, 1111–1116.

Newman, S.P., Jones, W., 1999. Comparative study of some layered hydroxide salts containing exchangeable interlayer anions. J. Solid State Chem. 148, 26–40.

Nishizawa, H., Yuasa, K., 1998. Preparation of anion exchangeable layered mixed basic salt $Ni_{1-x}Zn_{2x}(OH)_2(OCOCH_3)_{2x}nH_2O$ thin film under hydrothermal conditions. J. Solid State Chem. 141 (1), 229–234.

Noyan, I., Cohen, J., 1987. Residual Stress: Measurement by Diffraction and Interpretation. Springer Verlag, New York.

Oliveira, H.B., Wypych, F., 2016. Evaluation of layered zinc hydroxide nitrate and zinc/nickel double hydroxide salts in the removal of chromate ions from solutions. J. Solid State Chem. 243, 136–145.

Oswald, H.R., 1969. Crystal structure of cadmium copper hydroxide nitrate, $CdCu_3(OH)_6(NO_3)_2 \cdot H_2O$. Helv. Chim. Acta 52, 2369–2380.

Pertlik, F., Dunn, P.J., 1990. Crystal structure of alvanite, $(Zn,Ni)Al_4(VO_3)_2(OH)_{12} \cdot 2H_2O$, the first example of an unbranched zweier-single chain vanadate in nature. Neues Jahrb. Miner. Monatsh. 9, 385–392.

Prince, J., Montoya, A., Ferrat, G., Valente, J.S., 2009. Proposed general sol-gel method to pre-
   pare multimetallic layered double hydroxides: synthesis, characterization, and envisaged
   application. Chem. Mater. 21 (24), 5826–5835.

Qu, J., Zhang, Q., Li, X., He, X., Song, S., 2016. Mechanochemical approaches to synthesize lay-
   ered double hydroxides: a review. Appl. Clay Sci. 119 (2), 185–192.

Rathee, G., Awasthi, A., Sood, D., Tomar, R., Tomar, V., Chandra, R., 2019. A new biocompati-
   ble ternary layered double hydroxide adsorbent for ultrafast removal of anionic organic dyes.
   Sci. Rep. 9, 16225.

Rius, J., Plana, F., 1986. Magnesium aluminium sodium hydroxide sulfate carbonate hydrate.
   Neues Jahrb. Miner. Monatsh. 1986, 263–272.

Rives, V., 2001. In: Rives, V. (Ed.), Layered Double Hydroxides: Present and Future. Nova Sci-
   ence Publishers, New York.

Rodgers, K.A., Chisholm, J.E., Davis, R.J., Nelson, C.S., 1977. Motukoreaite, a new hydrated car-
   bonate, sulfate, and hydroxide of magnesium and aluminum from Auckland, New Zealand.
   Miner. Mag. 41, 389–390.

Rothbauer, R., Zigan, F., O'Daniel, H., 1967. Verfeinerung der Struktur des Bayerits,
   $Al(OH)_3$ Einschliesslich eines vorschlags fur die H-positionen. Z. Kristallogr. 125, 317–331.

Ruby, C., Aïssa, R., Géhin, A., Cortot, J., Abdelmoula, M., Génin, J.M., 2006. Green rusts synthe-
   sis by co-precipitation of FeII–FeIII ions and mass-balance diagram. C. R. Geosci. 338,
   420–432.

Rujiwatra, A., Kepert, C.J., Rosseinsky, M.J., 1999. The organo-pillared porous magnetic frame-
   work $Co_4(SO_4)(OH)_6(H_2NC_2H_4NH_2)_{0.5} \cdot 3H_2O$. Chem. Commun. 22, 2307–2308.

Ryu, S., Jung, H., Oh, J., Lee, J., Choy, J., 2010. Layered double hydroxide as novel antibacterial
   drug delivery system. J. Phys. Chem. Chem. Solids 71 (4), 685–688.

Saalfeld, H., Jarchow, O., 1968. Die kristallstruktur von Nordstrandit, $Al(OH)_3$. Neues Jahrb.
   Miner. Abh. 109, 185–191.

Saalfeld, H., Wedde, M., 1974. Refinement of the crystal structure of Gibbsite, $Al(OH)_3$. Zeitsch.
   Kristallogr. 139, 129–135.

Schlüter, J., Klaska, K.H., Friese, K., Adiwidjaja, G., Gebhard, G., 1997. Gordaite, $NaZn_4(SO_4)$
   $(OH)_6Cl \cdot 6H_2O$, a new mineral from the San Francisco Mine, Antofagasta, Chile. Neues Jahrb.
   Miner. Monatsh. 4, 155–162.

Schmetzer, K., Schnorrer-Köhler, G., Medenbach, O., 1985. Wülfingitem - ε-$Zn(OH)_2$ and simon-
   kolleite $Zn_5(OH)_8Cl_2H_2O$, two new minerals from Richelsdorf, Hesse, F.R.G. Neues Jahrb.
   Miner. Monatsh. 145, 145–154.

Serna, C.J., Rendon, J.L., Iglesias, J.E., 1982. Crystal-chemical study of layered $[Al_2Li(OH)_6]^+X^-$
   nH_2O. Clays Clay Miner. 30, 180–184.

Sherman, I.T. (Ed.), 2015. Layered Double Hydroxides (LDH): Synthesis, Characterization and
   Applications. Nova Science Publishers.

Shi, L., Li, D.Q., Wang, J.R., Li, S.F., Evans, D.G., Duan, X., 2005. Synthesis, flame-retardant
   and smoke-suppressant properties of a borate-intercalated layered double hydroxide. Clays
   Clay Miner. 53, 294–300.

Silva, M.L.N., Marangoni, R., Cursino, A.C.T., Schreiner, W.H., Wypych, F., 2012. Colorful and
   transparent poly(vinyl alcohol) composite films filled with layered zinc hydroxide salts, inter-
   calated with anionic orange azo dyes (methyl orange and orange II). Mater. Chem. Phys. 134,
   392–398.

Sotiles, A.R., Baika, L.M., Grassi, M.T., Wypych, F., 2019a. Cation exchange reactions in layered
   double hydroxides intercalated with sulfate and alkali cations $(A(H_2O)_6)[M_6^{+2}Al_3(OH)_{18}$
   $(SO_4)_2] \cdot 6H_2O$ (M^{+2} = Mn, Mg, Zn, A^+ = Li, Na, K). J. Am. Chem. Soc. 141, 531–540.

Sotiles, A.R., Baika, L.M., Grassi, M.T., Wypych, F., 2019b. Synthesis, characterization, thermal behavior and exchange reactions of new phases of layered double hydroxides with the chemical composition $[M_6^{+2}Al_3(OH)_{18}(SO_4)_2].(A(H_2O)_6)\cdot6H_2O$ (M^{+2} = Co, Ni; A = Li$^+$, Na$^+$, K$^+$). Appl. Clay Sci. 181, 105217.

Sotiles, A.R., Wypych, F., 2019. Converting Mn/Al layered double hydroxide anion exchangers into cation exchangers by topotactic reactions using alkali metal sulfate solutions. Chem. Commun. 55, 7824–7827.

Staal, L.B., Pushparaj, S.S.C., Forano, C., Prevot, V., Ravnsbaek, D.B., Bjerring, M., Nielsen, U.G., 2017. Competitive reactions during synthesis of zinc aluminum layered double hydroxides by thermal hydrolysis of urea. J. Mater. Chem. A 5, 21795–21806.

Stahlin, W., Oswald, H.R., 1970. Crystal structure of zinc hydroxide nitrate $Zn_5(OH)_8$ $(NO_3)_2.2H_2O$. Acta Crystallogr. B 26, 860–863.

Stamate, A.E., Pavel, O.D., Zavoianu, R., Marcu, I.C., 2020. Highlights on the catalytic properties of polyoxometalate-intercalated layered double hydroxides: a review. Catal. 10 (1), 57.

Stanimirova, T., 2019. Exchange reactions of zinc hydroxide-sulfate minerals in halide solutions. Appl. Clay Sci. 168, 396–408.

Stanimirova, T., Dencheva, S., Kirov, G., 2013. Structural interpretation of anion exchange in divalent copper hydroxysalt minerals. Clay Miner. 48, 21–36.

Stanimirova, T., Kerestedjian, T., Kirov, G., 2017. Dehydration and rehydration of Zn-hydroxy sulfate minerals with interrupted decorated hydroxide sheets. Appl. Clay Sci. 135, 16–26.

Stock, N., Biswas, S., 2012. Synthesis of metal-organic frameworks (MOFs): routes to various MOF topologies, morphologies, and composites. Chem. Rev. 112 (2), 933–969.

Szabados, M., Konya, Z., Kukovecz, A., Sipos, P., Palinko, I., 2019. Ultrasonically-assisted mechanochemical synthesis of zinc aluminate spinel from aluminium-rich layered double hydroxide. J. Solid State Chem. 272, 227–233.

Tang, S., Yao, Y., Chen, T.Y., Kong, D.Z., Shen, W., Lee, H.K., 2020. Recent advances in the application of layered double hydroxides in analytical chemistry: a review. Anal. Chim. Acta 1103, 32–48.

Tavares, S.R., Moraes, P.I.R., Capaz, R.B., Leitão, A.A., 2019. Novel 2D materials from exfoliation of layered hydroxide salts: a theoretical Study. Appl. Surf. Sci. 483, 762–771.

Tessier, C., Guerlou-Demourgues, L., Faure, C., Demourgues, A., Delmas, C., 2000. Structural study of zinc substituted nickel hydroxides. J. Mater. Chem. 10, 1185–1193.

Thomas, N., 2012. Mechanochemical synthesis of layered hydroxy salts. Mater. Res. Bull. 47, 3568–3572.

Uvarova, Y.A., Sokolova, E., Hawthorne, F.C., Karpenko, V.V., Agakhanov, A.A., Pautov, L.A., 2005. The crystal chemistry of the "nickelalumite"—group minerals. Can. Mineral. 43, 1511–1519.

Wang, Q., Astruc, D., 2020. State of the art and prospects in metal-organic framework (MOF)-based and MOF-derived nanocatalysis. Chem. Rev. 120 (2), 1438–1511.

Wang, Q., O'Hare, D., 2012. Recent advances in the synthesis and application of layered double hydroxide (LDH) nanosheets. Chem. Rev. 112, 4124–4155.

Wang, Y., Yan, D., El Hankari, S., Zou, Y., Wang, S., 2018. Recent progress on layered double hydroxides and their derivatives for electrocatalytic water splitting. Adv. Sci. 5 (8), 1800064.

Wei, M., Yuan, Q., Evans, D.G., Wang, Z., Duan, X., 2005. Layered solids as a 'Molecular Container' for pharmaceutical agents: L-tyrosine-intercalated layered double hydroxides. J. Mater. Chem. 15, 1197–1203.

Williams, G.R., Dunbar, T.G., Beer, A.J., Fogg, A.M., O'Hare, D., 2006a. 1: intercalation chemistry of the novel layered double hydroxides $[MAl_4(OH)_{12}](NO_3)_2 \cdot yH_2O$ (M = Zn, Cu, Ni and Co). 1: new organic intercalates and reaction mechanisms. J. Mater. Chem. 16, 1222–1230.

Williams, G.R., Dunbar, T.G., Beer, A.J., Fogg, A.M., O'Hare, D., 2006b. Intercalation chemistry of the novel layered double hydroxides $[MAl_4(OH)_{12}](NO_3)_2 \cdot H_2O$ (M = Zn, Cu, Ni and Co) 2: selective intercalation chemistry. J. Mater. Chem. 16, 1231–1237.

Williams, S.A., Khin, B.S., 1971. Chalcoalumite from Bisbee, Arizona. Miner. Rec. 2, 126–127.

Witzke, T., Pöllmann, H., Vogel, A., 1995. Struktur und synthese von $[Zn_{8-x}Al_x(OH)_{16}]$ $[(SO_4)_{x/2+y/2} \cdot Na_y(H_2O)_6]$. Zeitsch. Kristallogr. 9, S.252.

Work, W.J., Horie, K., Hess, M., Stepto, R.F.T., 2004. Definitions of terms related to polymer blends, composites and multiphase polymeric materials. Pure Appl. Chem. 76 (11), 1985–2007.

Wypych, F., Arizaga, G.G.C., Gardolinski, J.E.F.C., 2005. Intercalation and functionalization of zinc hydroxide nitrate with mono- and dicarboxylic acids. J. Colloid Interface Sci. 283 (1), 130–138.

Wypych, F., Satyanarayana, K.G. (Eds.), 2004. Clay Surfaces—Fundamentals and Applications. Vol. 1. Academic Press.

Wypych, F., Satyanarayana, K.G., 2005. Functionalization of single layers and nanofibers: a new strategy to produce polymer nanocomposites with optimized properties. J. Colloid Interface Sci. 285 (2), 532–543.

Wypych, F., Schöllhorn, R., 1992. 1T-MoS$_2$ a new metallic modification of molybdenum disulfide. J. Chem. Soc., Chem. Commun. 1386–1388.

Wypych, F., Solenthaler, C., Prins, R., Weber, T., 1999. Electron diffraction study of intercalation compounds derived from 1T-MoS$_2$. J. Solid State Chem. 144, 430–436.

Wypych, F., Bergaya, F., Schoonheydt, R.A., 2018. From polymers to clay mineral-polymer nanocomposites. In: Schoonheydt, R., Johnston, C., Bergaya, F. (Eds.), Surface and Interface Chemistry of Clay Minerals. vol. 9. (Chapter 10).

Xu, S.L., Chen, Z., Zhang, B., Yu, J., Zhang, F.Z., Evans, D.G., 2009. Facile preparation of pure CaAl-layered double hydroxides and their application as a hardening accelerator in concrete. Chem. Eng. J. 155, 881–885.

Yan, K., Wu, G., Jin, W., 2016. Recent advances in the synthesis of layered double-hydroxide-based materials and their applications in hydrogen and oxygen evolution. Energ. Technol. 4, 354–368.

Yang, Q.Z., Chang, Y.Y., Zhao, H.Z., 2013. Preparation and antibacterial activity of lysozyme and layered double hydroxide nanocomposites. Water Res. 47 (17), 6712–6718.

Yang, M., McDermott, O., Buffet, J.-C., O'Hare, D., 2014. Synthesis and characterisation of layered double hydroxide dispersions in organic solvents. RSC Adv. 4 (93), 51676–51682.

Yang, Z., Zhang, C., Zeng, G., Tan, X., Wang, H., Huang, D., Yang, K., Wei, J., Ma, C., Nie, K., 2020. Design and engineering of layered double hydroxide based catalysts for water depollution by advanced oxidation processes: a review. J. Mater. Chem. A 8, 4141–4173.

Zamarreno, I., Plana, F., Vasquez, A., Clague, D.A., 1989. Motukoreaite: a common alteration product in submarine basalts. Am. Miner. 74, 1054–1058.

Zegeye, A., Ona-Nguema, G., Carteret, C., Huguet, L., Abdelmoula, M., Jorand, F., 2005. Formation of hydroxysulphate green rust 2 as a single iron(II-III) mineral in microbial culture. Geom. J. 22, 389–399.

Zhang, F., Sun, M., Xu, S.L., Zhao, L., Zhang, B., 2008. Fabrication of oriented layered double hydroxide films by spin coating and their use in corrosion protection. Chem. Eng. J. 141, 362–367.

Zhang, G.H., Zhang, X.Q., Meng, Y., Pan, G.X., Ni, Z.M., Xia, S.J., 2020. Layered double hydroxides-based photocatalysts and visible-light driven photodegradation of organic pollutants: a review. Chem. Eng. J. 392, 123684.

Zhitova, E.S., Pekov, I.V., Chaikovskiy, I.I., Chirkova, E.P., Yapaskurt, V.O., Bychkova, Y.V., Belakovskiy, D.I., Chukanov, N.V., Zubkova, N.V., Krivovichev, S.V., Bocharov, V.N., 2019. Dritsite, $Li_2Al_4(OH)_{12}Cl_2 \cdot 3H_2O$, a new gibbsite-based hydrotalcite supergroup mineral. Miner. 9 (8), 492–506.

Zigan, F., Rothbauer, R., 1967. Neutronenbeugungmessungen am Brucit. Neues Jahrb. Miner. Monatsh. 4, 137–143.

Zimmermann, A., Jaerger, S., Zawadzki, S.F., Wypych, F., 2013. Synthetic zinc layered hydroxide salts intercalated with anionic azo dyes as fillers into high-density polyethylene composites: first insights. J. Polym. Res. 20, 224–234.